8－7　認知症(痴呆)

認知症は，いったん正常に発達した知能が後天的な脳の器質的障害により低下した状態をさす。認知症は脳血管性と変性性に大別され，変性性認知症としては**アルツハイマー型**が最も多い。認知症は記憶障害，見当識障害(場所や時間などがわからない)，判断障害を基本障害とし，不適切な感情，人格の変化を伴う。時に幻覚や妄想などの行動障害を伴うが必須ではない。日本では脳血管性認知症が多かったが，人口の高齢化に伴いアルツハイマー型認知症が増加している。**アルツハイマー型認知症の有病率**は1～5％と幅が広い。これは年齢が進むにつれて発現は急速に増加する(おおよそ5年ごとに倍加する)ためである。アルツハイマー型認知症の原因は代謝異常，アミロイド類前駆物質タンパク，プラーク関連タンパク，タウタンパク，亜鉛やアルミニウム等の代謝障害，アポリポタンパクの遺伝子多型の違いなど発症リスクを高める遺伝子などが示唆されているが，依然不明である。**脳血管性認知症を予防**するには，その原因となる生活習慣病を予防することが重要である。アルツハイマー型認知症の予防については不明であるが，廃用性による脳の機能低下を防ぐために，計算や運動など頭や体を使うことが有用とされている。またアルツハイマー型認知症にはドネペジル(商品名：アリセプト)が症状緩和や進行の緩徐化に効果を発揮することがある。またアルツハイマー型認知症のワクチンも開発されつつある。

日本では2004(平成16)年12月24日付けで，関連各学会においても2007(平成19)年までに痴呆の呼称が行政上「認知症」となった。

9 自　殺

自殺は世界的には15～34歳の年齢群で死亡原因の上位3位にあり，世界公衆衛生上の重大な問題となっている。自殺率は10万人につき15.1人とされ，老年期を除き圧倒的に男性が多い(男：女　3.5：1)。日本では，警察庁生活安全局の報告によると，中高年の自殺の増加に伴い，2003(平成15)年の自殺既遂者は3万4千人を越え，以後3万2～3千人前後で推移している。自殺未遂者は自殺既遂者の20倍以上になるといわれ，日本でも大きな社会問題となっている。同局の報告によると2003年度の自殺の原因・動機としては，「健康問題」が最も多く，「経済・生活問題」，「家庭問題」がこれに続いている。精神障害による自殺のなかでは，うつ病が最も多く(Pokorny, 1964)，その自殺は反復される傾向がある。先に述べた，統合失調症，精神作用薬物使用による精神および行動障害やPTSDも原因となり得る(表5－17, 別冊p.18)。

表5－17
■年齢階級別にみた不慮の事故による死亡の状況

自殺予防の1つとして，自殺の危険性が高い精神疾患である**うつ病**の有無を明らかにして，治療に結びつけることが挙げられる。うつ病は治る病気であることから，家族や職場でうつ病に関する教育を行い，うつ病の場合には早急に治療を受けさせるようにすることが重要である。「仕事の失敗から」，「借金を苦にして」，「人間関係に疲れて」などによるとされる自殺のかなりの部分は，適切な医療を受ければ治癒し得るうつ病によるものと考えられている。老年期の自殺予防には孤独感や疎外感をもたせないこと，何らかの役割を持たせることが有効とされている。また，一度自殺企図を

行った人は，繰り返す傾向があるので充分な注意が必要である(一度自殺を図って助かった人は二度と自殺しないというのは間違いである)。

〈吉田寿美子〉

10 その他の疾患

10−1 肝臓疾患

肝臓疾患の主要なものに**肝硬変**が挙げられる。肝硬変は肝細胞の壊死を伴う肝機能不全状態である。成因の大半を**ウイルス肝炎**が占め(C型肝炎約60％，B型肝炎約15％)，アルコール性が1割強である。

ウイルス肝炎には，A型，B型，C型などがある。**A型肝炎**は食物(生牡蠣など魚介類)・飲料水等からの経口感染により平均約30日の潜伏期ののち急激に発症するが，慢性化せず予後良好である。症状は，発熱，悪心・嘔吐，腹痛，全身倦怠感，黄疸などである。

B型肝炎は血液，唾液などを通して感染し，乳幼児が感染した場合は持続感染者(キャリア)となりやすいが，成人が感染した場合慢性化することはまれとされる。かつては出産時における母子感染等が多かったこともあり，B型肝炎ウイルスキャリアは推定120〜140万人いるが，昭和60年度から妊婦検診でHBs抗原検査を行い，子に対するワクチン投与などの適切な予防措置を講じたため(B型肝炎母子感染防止事業)，キャリアの数は減少している。

一方，**C型肝炎**は血液により感染し(輸血，入れ墨，注射器等)，高率に慢性化しキャリアとなる。日本には推定100〜200万人のキャリアがおり，そのうち一定の割合(6割という推定もある)が20年をかけて肝硬変に移行し，さらに肝がんへと移行する。したがって，C型慢性肝炎患者にはインターフェロンによりウイルスを駆除する治療等が必要となる。感染予防のためには，日常生活において剃刀，歯ブラシ，爪切り等の共用を避けることが重要である。

10−2 腎臓疾患

腎不全は死因第8位の疾患である(2007年)。腎不全は，慢性あるいは急性に腎機能障害が進行した状態で，治療法には**人工透析療法**，腎臓移植などがある。原因としては，原発性の**腎疾患**(糸球体腎炎など)によるもの，糖尿病などの全身疾患に伴うものなどがある。**糖尿病性腎症**による腎不全患者は新規人工透析患者の42.9％(第1位)，全人工透析患者(282,622人)の34.2％を占める(2008年)。そこで，糖尿病対策は腎不全患者を減らす大きな力となる。

10−3 消化器疾患

胃潰瘍，十二指腸潰瘍等の消化性潰瘍が挙げられるが，その病因について従来の酸分泌過多説に代わり，最近は**ヘリコバクター・ピロリ**(HP)菌が胃粘膜傷害を起こし酸の攻撃を受けやすくすることが重要視され，治療もHP除菌治療が保険適用になっ

The American Journal of Pathology, Vol. 179, No. 6, December 2011

DOI: 10.1016/j.ajpath.2011.08.023

Cell Injury, Repair, Aging, and Apoptosis

Glyoxalase I Retards Renal Senescence

Yoichiro Ikeda,* Reiko Inagi,* Toshio Miyata,† Ryoji Nagai,‡ Makoto Arai,§ Mitsuhiro Miyashita,§ Masanari Itokawa,§ Toshiro Fujita,* and Masaomi Nangaku*

From the Division of Nephrology and Endocrinology, Graduate School of Medicine, the University of Tokyo, Tokyo; the United Centers for Advanced Research and Translational Medicine,† Graduate School of Medicine, Tohoku University, Miyagi; the Department of Food and Nutrition,‡ Laboratory of Biochemistry and Nutritional Science, Japan Women's University, Tokyo; and the Tokyo Institute of Psychiatry,§ Tokyo, Japan*

Although kidney functions deteriorate with age, little is known about the general morphological alterations and mechanisms of renal senescence. We hypothesized that carbonyl stress causes senescence and investigated the possible role of glyoxalase I (GLO1), which detoxifies precursors of advanced glycation end products in the aging process of the kidney. We observed amelioration of senescence in GLO1-transgenic aged rats (assessed by expression levels of senescence markers such as p53, $p21^{WAF1/CIP1}$, and $p16^{INK4A}$) and a positive rate of senescence-associated β-galactosidase (SABG) staining, associated with reduction of renal advanced glycation end product accumulation (estimated by the amount of carboxyethyl lysine). GLO1-transgenic rats showed amelioration of interstitial thickening (observed as an age-related presentation in human renal biopsy specimens) and were protected against age-dependent decline of renal functions. We used GLO1 overexpression or knockdown in primary renal proximal tubular epithelial cells to investigate the effect of GLO1 on cellular senescence. Senescence markers were significantly upregulated in renal proximal tubular epithelial cells at late passage and in those treated with etoposide, a chemical inducer of senescence. GLO1 cellular overexpression ameliorated and knockdown enhanced the cellular senescence phenotypes. Furthermore, we confirmed the association of decreased GLO1 enzymatic activity and age-dependent deterioration of renal function in aged humans with GLO1 mutation. These findings indicate that GLO1 ameliorates carbonyl stress to retard renal senescence. ***(Am J Pathol 2011, 179:2810–2821; DOI: 10.1016/j.ajpath.2011.08.023)***

Prevention of aging and increase in longevity have long been dreamt of, and many hypotheses to explain the complex process of aging have been advanced. Primary somatic cells grown *in vitro* do not proliferate indefinitely; rather, after a period of rapid proliferation, the cell division rate slows and ultimately ceases altogether, with the cells becoming unresponsive to mitogenic stimuli, a phenomenon known as replicative senescence or Hayflick's limit. Senescent cells have characteristic features, notably the accumulation of advanced glycation end products (AGEs), wide changes in gene expression (including up-regulation of cell cycle regulators such as p53, $p21^{WAF1/CIP1}$, and $p16^{INK4A}$), and increased senescence-associated β-galactosidase (SABG) activity.[1,2] Irrespective of chronological aging, cells exhibiting the combination of these features are considered to be in premature senescence.[3]

The mechanisms of senescence have been widely investigated. The free radical theory of aging proposes that endogenous reactive oxygen species (ROS) generated in cells result in cumulative damage and subsequent senescence.[4] However, attempts to induce longevity by eliminating oxidative stress in genetically engineered mice have been unsuccessful, suggesting that involvement of free radicals is not a sufficient explanation of senescence.[5,6] Another possible mechanism accounting for senescence is carbonyl stress and AGE formation. Carbonyl compound derivatives are generated by carbohydrate oxidation and glycolysis.[7] AGE formation is caused by carbonyl compound derivatives as protein modification precursors.[8,9] Among the many carbonyl derivatives, the most reactive are thought to be glyoxal and methylglyoxal, which act as protein modification precursor and synergistically contribute to AGE formation.[10] Serum AGE levels were reported to increase with age in a large cohort of normal subjects, and correlated well with levels of established markers of oxidative stress and inflammation.[11] AGE accumulation is associated with the development of age-related diseases, such as diabetes

Supported by Grant-in-Aid for Scientific Research 22590880 (R.I.) and 2139036 (M.N.) from the Japan Society for the Promotion of Science.

Accepted for publication August 24, 2011.

Address reprint requests to Masaomi Nangaku, M.D., Ph.D., Division of Nephrology and Endocrinology, University of Tokyo School of Medicine, 7-3-1 Hongo, Bunkyo-ku, Tokyo, Japan, 113-8655. E-mail: mnangaku-tky@umin.ac.jp.

mellitus, Alzheimer's disease, and atherosclerosis,[12,13] and carbonyl stress is likely to be, at least in part, a cause rather than a consequence of the aging process.[14]

Assuming that glyoxal and methylglyoxal accelerate senescence, acceleration of their decomposition might prevent organs from aging. Both compounds are rapidly decomposed by GLO1 and GLO2, the two enzymes of the glyoxalase (GLO) system. GLO1 catalyzes the conversion of glyoxal and methylglyoxal and reduces glutathione (GSH) to *S*-D-lactoyl-GSH; it is expressed ubiquitously in most tissues, serving as the rate-limiting enzyme of methylglyoxal catabolism.[15–18] In one study, overexpression of GLO1 protected the kidney against ischemia and reperfusion injury by inhibiting the formation of intracellular methylglyoxal adducts and oxidative stress.[19]

In the present study, we investigated the possible roles of carbonyl stress and of GLO1 in renal senescence.

Materials and Methods

Animal Experimental Protocol

Male Wistar rats [wild type (WT)] and male transgenic Wistar rats overexpressing human GLO1 (Tg-GLO1) were used. The Tg-GLO1 rats were generated as described previously.[19,20] Rats 10 weeks of age or 14 months of age were fed a standard moderate-fat diet and tap water *ad libitum* (32 total; $n = 8$ for each age/genotype combination). Food intake was monitored from 2 weeks before sacrifice, and body weight was measured at the time of sacrifice. Systolic blood pressure of awake rats was measured by the tail-cuff method using a Softron BP-98A unit (Softron, Tokyo, Japan). All animal experiments were performed in accordance with the NIH guidelines (7th edition) for use and care of laboratory animals and were approved by the local ethical committees.

Histological Analysis for Age-Related Morphological Change

Tissues from rat and human kidney were fixed in formalin solution and paraffin-embedded. Sections (3 μm thick) were stained with Masson's trichrome staining for rat tissue or with Azan staining for human tissue. Interstitial thickness was measured at a magnification of ×600 as the smallest width of the interstitial area (stained blue) between two intact tubules in 20 sites selected randomly from six fields of renal cortex. This smallest-width measurement was chosen to account for tubules not perpendicular to the cutting plane.

Human renal biopsy specimens obtained from patients admitted to the University of Tokyo Hospital were reviewed with institutional permission (Graduate School of Medicine, University of Tokyo, Permission no. 2671) and with informed consent. Exclusion criteria included confounding factors such as proteinuria [urinary protein > 1 g/g creatinine (Cr)], renal dysfunction (estimated glomerular filtration rate eGFR < 60 mL/min per 1.73 m^2), interstitial nephritis of primary or secondary origin, and diabetes mellitus. The human renal biopsy specimens were mostly from patients with IgA nephropathy, and comparison of glomerular change was not performed because this variable was dependent on disease activity. In all, 22 patients were recruited.

Chemical Analysis

Creatinine concentration was measured by the enzyme method using a Kainos Cre kit (Kainos Laboratories, Tokyo, Japan). Protein concentration was measured by the Lowry method, using DC protein assay reagents (Bio-Rad Laboratories, Hercules, CA). Rat blood or urine samples collected for 24 hours in metabolic cages were used after centrifugation for 5 minutes at 3000 × *g*. Blood glucose level was measured using an automated blood glucose meter (Glutest Ace; Sanwa Chemical, Nagoya, Japan). Blood insulin level was measured using a rat insulin ELISA kit (AKRIN-010T; Shibayagi, Gunma, Japan). HbA1c was measured by high performance liquid chromatography.

Determination of GLO1 Activity and GSH Concentrations

Renal cortex of rats (30 mg) or 10^4 to 10^5 renal proximal tubular epithelial cells (RPTECs) were homogenized in, respectively, 0.5 mL or 50 μL of sodium phosphate buffer, pH 7.0, containing 0.02% Triton X-100 surfactant, then sonicated for 1 minute, and finally centrifuged at 20,000 × *g* for 1 minute at 4°C. The supernatant was used for assessment of GLO1 activity by spectrophotometry, as described previously.[21] GSH concentration in renal cortical homogenates from rats was measured with Bioxytech GSH-412 assay reagent (Oxis International, Portland, OR). Values were adjusted by the protein concentration of the same sample.

Determination of Total Superoxide Dismutase Activity

Total superoxide dismutase (SOD) activity in renal tissue was determined using a superoxide dismutase assay kit (Cayman Chemical, Ann Arbor, MI). Sample preparation and measurement were performed according to the manufacturer's instructions. Values were adjusted by the protein concentration of the same sample.

Senescence-Associated β-Galactosidase Staining Assay

Staining for senescence-associated β-galactosidase (SABG), one of the senescence markers, was performed using a Chemicon cellular senescence assay kit (Millipore, Billerica, MA). For tissue staining, frozen 15-μm kidney sections were incubated for 5 hours. The SABG-positive (blue-stained) areas of whole renal cortex were measured at ×100 magnification. The SABG-positive rate of tissue was calculated using ImageJ software (version 1.38) (NIH, Bethesda, MD) with adequate setting of threshold and computed measurement of area fraction,

obtained after analyzing particles. Eight areas of each kidney section were used for statistical assessment. For costaining of SABG staining and γ-GTP staining or immunohistochemical staining, frozen 10-μm kidney sections were used. SABG staining, with 12 hours of incubation, was performed prior to immunohistochemical staining.

Immunoblot Analysis

Proteins were separated by 10% to 15% SDS-PAGE under reducing conditions. Monoclonal mouse anti-p53 IgG (Calbiochem Ab-1, 1:100; EMD Chemicals, Cambridge, MA), monoclonal mouse anti-$p16^{INK4A}$ IgG (sc-1661, 1:200; Santa Cruz Biotechnology, Santa Cruz, CA), monoclonal mouse anti-CEL IgG (1:100),[22] and polyclonal rabbit anti-β actin IgG (A2066, 1:1000; Sigma-Aldrich, St. Louis, MO) were used as primary antibodies, and horseradish peroxidase-conjugated anti-mouse or anti-rabbit IgG (170–6516 for anti-mouse and 170–6516 for anti-rabbit, 1:1000; Bio-Rad Laboratories) were used as secondary antibodies. The ECL Plus Western blotting system (GE Healthcare, Piscataway, NJ) was used for detection. Reproducibility was confirmed in three independent experiments; representative data are presented in the figures.

Immunohistochemistry

The following primary antibodies were used: polyclonal rabbit anti-GLO1 IgG (12 μg/mL, obtained from immunization against synthetic peptide of rat GLO1, GIAVPDVYEA, which cross-reacts with the human GLO1 epitope, GIAVPDVYSA); anti-aquaporin2 (AQP2) IgG (Chemicon AB3274) from Millipore; anti-p53 IgG (sc-6243), monoclonal mouse anti-$p21^{WAF1/CIP1}$ IgG (sc-6246), and anti-$p16^{INK4A}$ IgG (sc-1661) from Santa Cruz Biotechnology; and anti-calbindin-D-28K IgG (c-9848) from Sigma-Aldrich. Polyclonal horse biotinylated anti-mouse IgG antibody or polyclonal goat anti-rabbit IgG (Vector Laboratories, Burlingame, CA) was used as secondary antibody. Reproducibility was confirmed in three independent experiments; representative data are reported in the results.

Real-Time Quantitative PCR

The primers used for real-time quantitative PCR were as follows: human GLO1 5′-ATTCGGTCATATTGGAATTGC-3′ (forward), 5′-TTCAATCCAGTAGCCATCAGG-3′ (reverse); human p53 5′-CCTCACCATCATCACACTGG-3′ (forward), 5′-TCTGAGTCAGGCCCTTCTGT-3′ (reverse); human $p21^{WAF1/CIP1}$ 5′-TGGAGACTCTCAGGGTCGAAA-3′ (forward), 5′-GGCGTTTGGAGTGGTAGAAATC-3′ (reverse); human $p16^{INK4A}$ 5′-CAACGCACCGAATAGTTACG-3′ (forward), 5′-AGCACCACCAGCGTGTC-3′ (reverse); human β-actin 5′-TCCCCCAACTTGAGATGTATGAAG-3′ (forward), 5′-AACTGGTCTCAAGTCAGTGTACAGG-3′ (reverse); rat p53 5′-CCTCAATAAGCTGTTCTGCC-3′ (forward), 5′-AAAAGTCTGCCTGTCGTCCA-3′ (reverse); rat $p21^{WAF1/CIP1}$ 5′-ACGTGGCCTTGTCGCTGTCTT-3′ (forward), 5′-TAAGGCAGAAGATGGGGAAGAG-3′ (reverse); rat $p16^{INK4A}$ 5′-ACGAGGTGCGGGCACTG-3′ (forward), 5′-TTGACGTTGCCCATCATCATC-3′ (reverse); rat β-actin 5′-CTTTCTACAATGAGCTGCGTG-3′ (forward), 5′-TCATGAGGTAGTCTGTCAGG-3′ (reverse); rat Mn-SOD 5′-CCGAGGAGAAGTACCACGAG-3′ (forward), 5′-GCTTGATAGCCTCCAGCAAC-3′ (reverse). Amplification specificity was verified by agarose gel electrophoresis of the PCR products. Expression data were normalized to β-actin using the ΔΔCt method.

Cell Culture

Primary human RPTECs derived from a 27-year-old woman of European origin were purchased from Clonetics (Walkersville, MD). The cells were cultured with renal epithelial basal medium (Clonetics). Early- and late-passage cells were compared at passages 3 and 10, respectively, and cells of passage 3 to 4 were used for transfection experiments. Confluent RPTEC monolayers were passaged at 1:4. Each experiment with RPTECs was performed three or more times independently.

Transfection

cDNA of human GLO1 (555 bp) was obtained using the following primers: 5′-CAGGCTAGCCATGGCAGAACCGCAGCC-3′ (forward), 5′-GGAGAATTCTCACAGCACTACATTAAG-3′ (reverse). Plasmid vector pcDNA3.1(−) (Invitrogen, Carlsbad, CA) was used for overexpression of GLO1. GLO1 containing pcDNA3.1(−) was constructed by inserting the complete human form GLO1 cDNA into the EcoRI and NheI sites. For overexpression experiments, 400 ng/cm^2 of GLO1-containing vector or empty vector was transfected into RPTECs by 5 hours of incubation with Lipofectamine 2000 transfection reagent (Invitrogen). Cells were exposed to 1 μmol/L etoposide for 24 hours if necessary. Transfection efficiency was confirmed by transfection of LacZ-containing vector followed by *in situ* β-galactosidase staining solution, using empty vector as control.

Knockdown Study

Knockdown study was performed using Stealth Select RNAi purchased from Invitrogen. Sequences for GLO1 were as follows: 5′-UUAGCGUCAUUCCAAGAACUCUAGU-3′ (siRNA 1), 5′-AAUCCAGUAGCCAUCAGGAUCUUGA-3′ (siRNA 2). Stealth RNAi negative control (universal negative control siRNA) from Invitrogen was used as scrambled siRNA. Knockdown efficiency was confirmed by real-time quantitative PCR with primers of human GLO1.

Cellular Proliferation and Viability Test

The number of viable cells was determined using a colorimetric MTS formazan assay with CellTiter 96 AQ_{ueous} One Solution cell proliferation assay (Promega, Madison, WI). Cells (10^3) were seeded with renal epithelial basal medium, with or without etoposide exposure.

For the lactate dehydrogenase (LDH) assay, 10^4 cells at early or late passage with or without etoposide exposure were seeded into each well of a 24-well plate with renal epithelial basal medium and were incubated for 24 hours. Cells were lysed with 0.1% Triton X-100 surfactant, and 2 μL of cell lysate and 200 μL of culture medium were used for each measurement. LDH activity was measured using a Kainos LDH kit (Kainos Laboratories).

Bromodeoxyuridine (BrdU) uptake was measured using a BrdU detection kit III (Roche Diagnostics, Indianapolis, IN). Cells (10^4) cells at passage 3 were seeded in each well of a 96-well plate and were cultured with serum-free Dulbecco's modified Eagle's medium for 24 hours, with etoposide added after transfection if necessary.

γ-Glutamyl Transpeptidase Staining

γ-Glutamyl transpeptidase (GTP) staining was performed according to the method of Rutenburg et al.[23] Duration of incubation for staining was 10 minutes at room temperature. No fixation was done before staining.

Immunofluorescence Study

Cells were fixed in 50% methanol/50% acetone and then were incubated with anti-CEL antibody (KNH-30; TransGenic, Kobe, Japan) as a primary antibody. Fluorescein isothiocyanate-conjugated polyclonal rabbit anti-mouse IgG (F0261; Dako, Glostrup, Denmark) was used as a secondary antibody. Nuclei were then counterstained with Hoechst 33258 dye (B2883; Sigma-Aldrich).

Renal Function and GLO1 Mutation in Human Schizophrenia Patients

For determination of eGFR, we used data from patients with schizophrenia whose GLO1 genotype had been established previously,[24] with permission and informed consent. The local human ethics committee approved all protocols involving patients, and informed written consent was obtained from every patient before enrollment. Three patients had the GLO1 frameshift mutation, with GLO1 activity half that of the nonmutant form,[24] and 15 age-matched control patients with WT GLO1 were randomly selected. All medical charts were reviewed for blood pressure, body weight, body height, urinary testing (hematuria, proteinuria), and medication. The eGFR was calculated using the following formula, which estimates GFR in a Japanese population[25]: $eGFR = 194 \times Cr^{-1.094} \times Age^{-0.287}$ ($\times$ 0.739 if female).

Statistical Analysis

Data are expressed as means ± SD. Statistical differences were assessed using the unpaired Student's *t*-test or single-factor analysis of variance. Significant differences determined on analysis of variance were tested by post hoc comparison using Tukey's method. Values of $P < 0.05$ were considered statistically significant. In analysis of human renal biopsy, the slope of interstitial thickness against age was calculated by linear regression analysis with Spearman's rank correlation coefficient.

Results

Amelioration of Senescent Status in Aged Kidneys of Tg-GLO1 Rats

To study the biological roles of carbonyl stress and GLO1 in renal senescence, we used young (10-week-old) and aged (14-month-old) Tg-GLO1 and WT rats (32 total; $n = 8$ for each age/genotype combination).[19,20] No significant differences were seen between the WT and Tg-GLO1 groups, either young or aged, in body weight, food intake per weight, or systolic blood pressure (Table 1). Levels of random (nonfasting) blood glucose did not significantly differ between WT and Tg-GLO1 rats during the experimental period. Normal glucose metabolism in the experimental animals was confirmed by measurements of fasting blood glucose, fasting blood insulin, insulin resistance, and HbA1c. The HOMA-IR (homeostasis model of assessment-insulin resistance) index of insulin resistance was calculated by multiplying fasting blood glucose and fasting blood insulin, then dividing by 405. All of these parameters were equivalent between aged WT and Tg-GLO1 rats (Figure 1, A–E). Similarly, levels of renal cortex GSH, an essential cofactor of GLO1, did not significantly differ between them (Figure 1F). To eliminate the effect of antioxidants, which may ameliorate senescence phenotypes by decreasing ROS levels, total superoxide dismutase (SOD) activity in renal tissue was measured. Total SOD activity was not significantly changed by GLO1 overexpression in either young or aged rats (Figure 1G). In addition, transcript levels of

Table 1. Body Weight, Food Intake, and Systolic Blood Pressure of Young and Elderly Wild-Type and Transgenic Rats

Characteristics	Young		Elderly	
	WT	Tg-GLO1	WT	Tg-GLO1
Body weight (g)	330 ± 17	330 ± 26	490 ± 56*	480 ± 54*
Chow intake (mg/day per g weight)	43 ± 13	42 ± 14	39 ± 12	42 ± 14
Systolic blood pressure (mmHg)	106 ± 4	104 ± 5	106 ± 11	104 ± 9

Significant differences were found in body weight in elderly compared with young rats, but no significant differences were found in those of the same age. No significant differences were observed in food intake or systolic blood pressure; $n = 8$ in each of the four categories.
* $P < 0.01$ versus young WT.

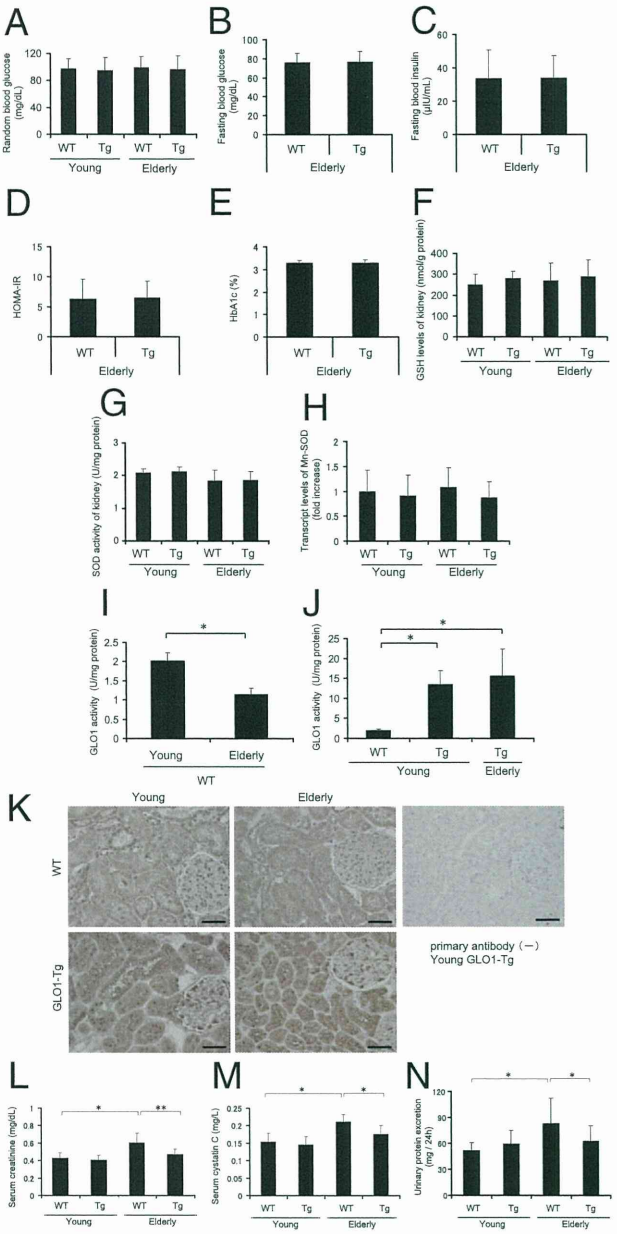

Figure 1. Characteristics of GLO1-overexpressing aged rats and amelioration of senescence-associated renal dysfunction and urinary protein excretion. No significant differences were observed between young and aged WT and Tg-GLO-1 rats for random (nonfasting) blood glucose levels (**A**), for levels of GSH, an essential cofactor of GLO1, in renal cortex lysate (data adjusted by protein concentration) (**F**), for total SOD activity of renal cortex lysate (data adjusted by protein concentration) (**G**), and for relative transcript levels of Mn-SOD (determined by real-time quantitative RT-PCR, with the value for young WT rats set as 1) (**H**). No significant differences were observed between aged WT and Tg-GLO-1 rats for fasting blood glucose levels (**B**), for fasting blood insulin levels (**C**), for HOMA-IR (calculated by multiplying fasting blood glucose and fasting blood insulin, then dividing by 405) (**D**), and for blood HbA1c levels (**E**). **I:** GLO1 activity of renal cortex lysate of WT animals decreased in an age-dependent manner. Data were adjusted by protein concentration. $^{*}P < 0.01$. **J:** GLO1 activity of renal cortex lysate in Tg-GLO1 rats was markedly higher than that in WT rats, and did not show an age-dependent decrease. Data were adjusted by protein concentration. $^{*}P < 0.01$ versus young WT rats. **K:** Distribution of GLO1 in rat kidney, shown in representative micrographs of immunohistochemical staining of GLO1 in the rat renal cortex. GLO1 was expressed ubiquitously in the kidney of both WT and Tg-GLO1 rats. Methyl Carnoy's fixed specimens (4 μm thick) were counterstained with hematoxylin. Original magnification = ×400. Scale bars: 50 μm. **L:** Serum creatinine levels determined by enzymatic assay indicate that the age-dependent deterioration of renal function was ameliorated by GLO1 overexpression. $^{*}P < 0.01$; $^{**}P < 0.05$. **M:** Serum cystatin C levels indicate that the age-dependent deterioration of renal function was ameliorated by GLO1 overexpression. $^{*}P < 0.01$. **N:** An age-dependent increase in proteinuria was prevented by GLO1 overexpression. Urine was collected for 24 hours using metabolic cages. $^{*}P < 0.05$.

manganese SOD (Mn-SOD, or SOD2) in kidney were measured by quantitative RT-PCR; Mn-SOD regulates only mitochondrial production of ROS because it is present only in mitochondria. No significant differences in Mn-SOD expression were observed between young and aged groups of WT and Tg-GLO1 rats (Figure 1H).

In WT rats, GLO1 activity was significantly decreased with age, to 0.55-fold the level in young rats (Figure 1I). GLO1 activity of young Tg-GLO1 rats showed a 6.3-fold increase, compared with young WT rats, but did not show an age-dependent decrease (Figure 1J). Immunohistochemical analysis showed that GLO1 was ubiquitously expressed with the same distribution pattern in the kidneys of both young and aged WT rats (Figure 1K). In contrast to the comparison in WT rats which showed age-dependent weakening of signal intensity, GLO1 signal intensity in Tg-GLO1 did not change with aging. Age-dependent deterioration of renal function, as estimated by serum creatinine, cystatin C levels, and urinary protein excretion, were markedly ameliorated by overexpression of GLO1 (Figure 1, L–N).

We assessed renal senescence status in WT and Tg-GLO1 rats by SABG staining. SABG was positive only in the tubular cells of aged rats; glomerular cells remained negative (Figure 2A). The functional improvement in renal senescence described above in Tg-GLO1 rats was associated with a decrease in SABG-positive rates in cortical tubular cells. Amelioration of senescence was confirmed by quantitative analysis of the SABG-positive rate, which was lower in the kidneys of aged Tg-GLO1 rats, compared with aged WT rats (Figure 2B). No significant differences were observed between the kidneys of young Tg-GLO1 and WT rats. To determine which segments of tubules are positive for SABG staining, we performed costaining of SABG and γ-GTP (a marker of proximal tubular cells), calbindin-D-28K (a marker of distal tubules and connecting tubules), or aquaporin2 (AQP2; a marker of connecting tubules and collecting ducts) (Figure 2, C–E). All segments had a propensity toward senescence, with no preponderance in specific tubular segments. The elevated transcript levels of senescence markers such as p53, $p21^{WAF1/CIP1}$, and $p16^{INK4A}$ in aged rats were significantly suppressed by GLO1 overexpression, compared with aged WT rats, whereas no significant differences were observed between the young groups (Figure 2F). Immunohistochemistry for the senescence markers showed that the nuclei of renal cortical tubules of aged WT rats were stained positive (in staining for p53, cytosol was also positive); these positive staining levels were markedly reduced in aged Tg-GLO1 rats (Figure 2G). Similar results were obtained by immunoblot analysis of renal cortex lysate for p53 and $p16^{INK4A}$. Protein expression level of p53 and $p16^{INK4A}$ in the young rats was undetectable; however, the increased expression of p53 and $p16^{INK4A}$ with age was reduced by GLO1 overexpression (Figure 2, H and I). In parallel with this suppression of senescence markers, age-dependent accumulation of carboxyethyl lysine (CEL) in the renal cortex was markedly suppressed by overexpression of GLO1 (Figure 2J).

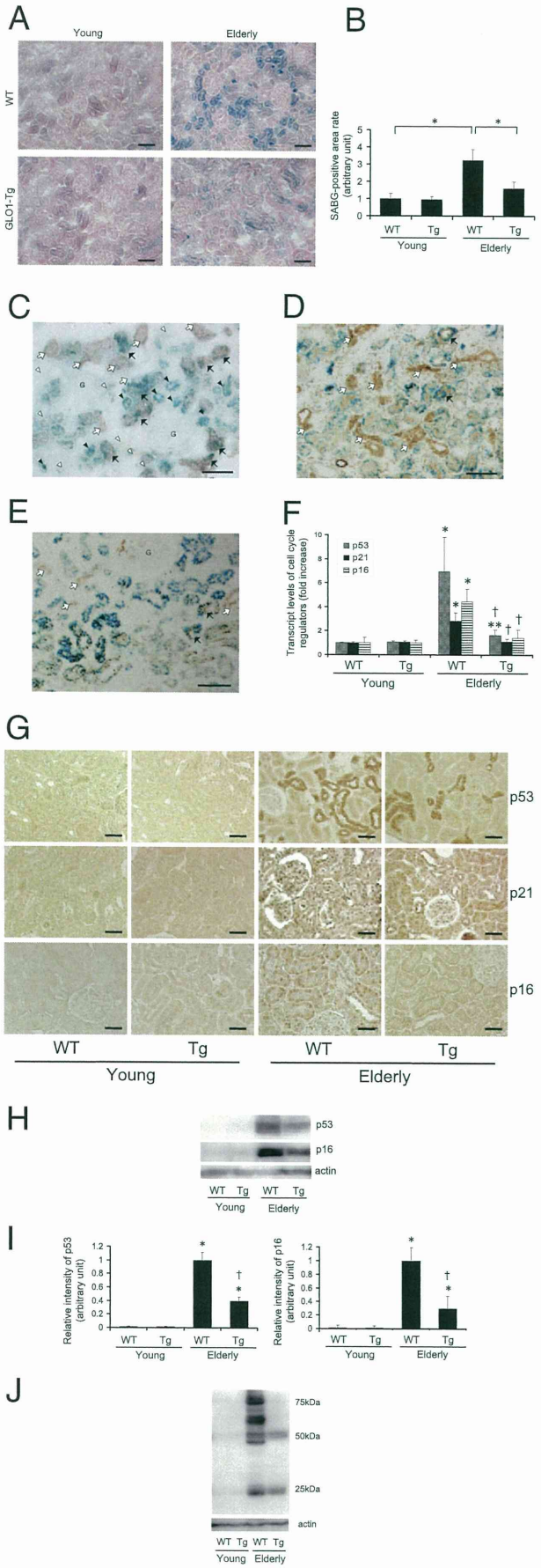

Age-Related Morphological Changes in the Renal Interstitium

To investigate whether amelioration of senescence markers and physiological parameters by overexpression of GLO1 was associated with improvement of pathological changes, we first assessed age-related morphological changes in human renal senescence, with a particular focus on tubulointerstitial changes (Figure 3A), on the basis that SABG staining was observed primarily in the tubules in aged rats. Review of specimens (mostly IgA nephropathy specimens with Azan staining) from 22 patients whose renal functions were preserved (eGFR of 80.4 ± 3.5 mL/min per 1.73m^2 and urinary protein excretion of 0.76 ± 0.21 g/day) showed an age-dependent increase in the thickness of the interstitium (Figure 3B). Linear regression analysis showed a strongly positive Pearson's correlation coefficient between age and the thickness of the renal peritubular interstitium (slope, 0.044 μm/year; $r^2 = 0.91$, $P < 0.01$).

In accord with the findings in humans, we observed tubulointerstitial morphological changes in aged rats. These changes were significantly decreased in aged Tg-GLO1 rats (Figure 3, C and D).

Figure 2. GLO1-overexpressing aged rats showed morphological amelioration in senescence-associated alterations of kidney. **A:** Light micrographs of rat renal cortex with SABG staining showing senescent tubular cells in aged WT rats. The number of senescent tubules was reduced by overexpression of GLO1. Frozen tissue specimens (15 μm thick) were counterstained with Nuclear Fast Red. Original magnification: ×100. Scale bars: 100 μm. Blue indicates SABG-positive cells. **B:** Quantitative analysis of SABG-positive area. The positive rate was calculated by dividing the positive area by the total area in each field and is expressed as fold increase, relative to the level of young WT rats. *$P < 0.01$. **C:** Representative light micrographs of renal cortex of aged WT rat, costained with SABG (blue) and γ-GTP (pale red). **Black arrows** mark senescent proximal tubular cells; **white arrows** mark nonsenescent proximal tubular cells. **Black arrowheads** mark senescent nonproximal tubular cells; **white arrowheads** mark nonsenescent nonproximal tubular cells. The letter G marks the glomerulus. Frozen specimens were examined without counterstaining. Original magnification = ×200. Scale bar = 100 μm. **D:** Representative light micrographs of renal cortex of aged WT rat costained with SABG (blue) and calbindin-D-28K. **Black arrows** mark senescent distal tubules-connecting tubules; **white arrows** mark nonsenescent distal tubules-connecting tubules. Frozen specimens were counterstained with hematoxylin. Original magnification = ×200. Scale bar = 100 μm. **E:** Representative light micrographs of renal cortex of aged WT rat costained with SABG (blue) and AQP2. **Black arrows** mark senescent connecting tubules-collecting ducts; **white arrows** mark nonsenescent connecting tubule-collecting ducts. The letter G marks the glomerulus. Frozen specimens were counterstained with hematoxylin. Original magnification = ×200. Scale bar = 100 μm. **F:** Relative transcript levels of p53, p21$^{WAF1/CIP1}$, and p16^{INK4A} were determined by real-time quantitative RT-PCR. All were significantly elevated in aged WT. This age-dependent increase was significantly reduced by overexpression of GLO1. The values for young WT rats were set as 1. *$P < 0.01$; **$P < 0.05$ versus young WT rats; †$P < 0.01$ versus aged WT rats. **G:** Representative micrographs of immunohistochemistry staining for p53, p21$^{WAF1/CIP1}$, and p16^{INK4A} in the rat renal cortex. In each staining, aged WT tissue exhibited marked increases in positive area in tubules. The extent of positive areas was significantly decreased by overexpression of GLO1. Methyl Carnoy's fixed specimens (4 μm thick) were counterstained with hematoxylin. Original magnification = ×400. Scale bars: 50 μm. **H:** Protein immunoblot of p53 and p16^{INK4A} of renal cortex lysate. Elevation of p53 and p16^{INK4A} in aged WT rats was attenuated by overexpression of GLO1. Actin served as a control. **I:** Densitometric quantification of p53 and p16^{INK4A} immunoblot. The values for aged WT rats were set as 1. *$P < 0.05$ versus young WT rats; †$P < 0.05$ versus aged WT rats. **J:** Protein immunoblot of CEL of renal cortex lysate indicates amelioration of carbonyl stress by GLO1 overexpression. Actin served as a control. Many bands were detected as CEL-modified protein, indicating that AGEs were accumulated in renal cortex.

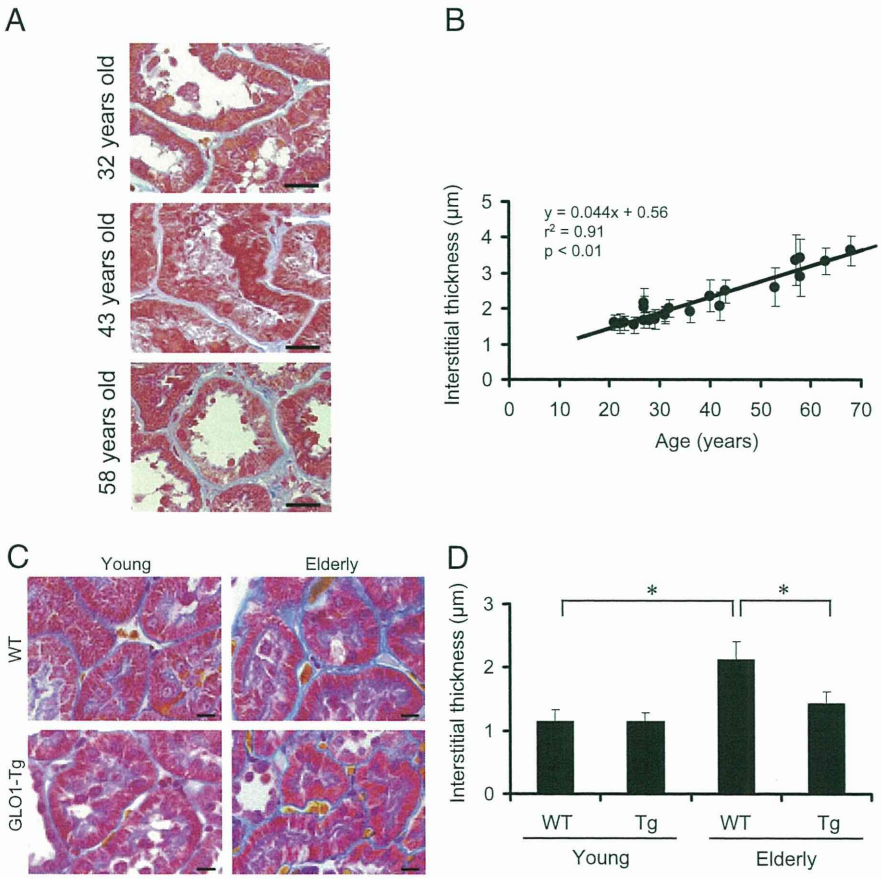

Figure 3. Interstitial thickening was demonstrated to be an age-related morphological change in human and rat kidney. **A:** Representative figures of human renal biopsy. Specimens were Azan-stained. Proximal tubular epithelial cells stain red and interstitium stains blue. The interstitial areas were thickened in an age-dependent manner. Original magnification = ×600. Scale bars: 20 μm. **B:** Correlation between age and interstitial thickness. The thickness of renal interstitia (blue) was measured under high-power magnification (×600). Each dot on the univariate linear regression line represents mean thickness (μm); error bars indicate ± SD. The calculation method is described under *Materials and Methods*. **C:** Light micrographs of rat renal cortex. Formalin-fixed specimens (3 μm thick) were stained with Masson's trichrome staining. Proximal tubular epithelial cells with brush borders stain red; interstitial areas stain blue (as for the human renal biopsy). The interstitial areas were thickened with age. This age-dependent thickening was attenuated by GLO1 overexpression. Original magnification = ×600. Scale bars: 10 μm. **D:** Quantitative histological analysis indicates that GLO1 overexpression ameliorated age-dependent interstitial thickening. $^{*}P < 0.01$; $^{**}P < 0.05$.

Carbonyl Stress and Cellular Senescence in Primary Cultured Tubular Cells

To confirm the significance of carbonyl compound in age-related alterations in tubular cells, we used primary cultured human RPTECs. First, we investigated the senescence status of RPTECs at early and late passage (passage 3 and 10, respectively). Cell proliferation estimated by the MTS assay showed that RPTECs reached replicative senescence at late passage (Figure 4A). Treatment of early-passaged cells with 1 μmol/L etoposide, a chemical senescence inducer, successfully induced replicative senescence, as was observed in late-passaged cells (Figure 4A). The LDH assay revealed no significant differences in cell viability among the three groups (Figure 4B). The cultured cells retained the phenotypes of proximal tubular cells, as evaluated by γ-GTP staining, a specific marker of proximal tubular cells. In contrast, γ-GTP was negative in rat renal fibroblasts (Figure 4C).

We then assessed the change in expression levels of cellular senescence markers in RPTECs at late passage or by etoposide treatment. The number of SABG-positive cells was significantly increased in late-passaged RPTECs and in early-passaged RPTECs treated with etoposide, compared with untreated early-passaged cells, verifying our assumption that the premature senescence induced by this chemical inducer closely mimics cellular senescence (Figure 5, A and B). We further assessed the changes in other senescence markers in the three groups of RPTECs. Transcriptional levels of p53, $p21^{WAF1/CIP1}$, and $p16^{INK4A}$ were significantly increased in late-passaged RPTECs and etoposide-treated early-passaged RPTECs, compared with untreated early-passaged RPTECs (Figure 5C). Immunoblot analysis followed by densitometry revealed the up-regulation of p53 at the protein level in RPTECs in association with replicative senescence (Figure 5, D and E). Immunofluorescent microscopy showed that late-passaged and etoposide-treated early-passaged cells showed accumulation of CEL, an indicator of carbonyl stress status, but untreated early-passaged cells did not (Figure 5F).

Beneficial Effect of GLO1 on Senescence of Tubular Cells

We next used RPTECs treated with etoposide for functional studies. First, we performed gain-of-function studies using early-passaged RPTECs overexpressing human GLO1, which is a detoxifying enzyme of reactive carbonyl compounds, including methylglyoxal. Transfection efficiency in RPTECs as estimated using LacZ expression as a reporter gene was 87 ± 6%, and GLO1 activity was up-regulated by 14 ± 2-fold in GLO1-transfected cells, compared with empty vector-transfected cells (Figure 6A). Overexpression of GLO1 did not change the basal expression level of SABG in these transfectants.

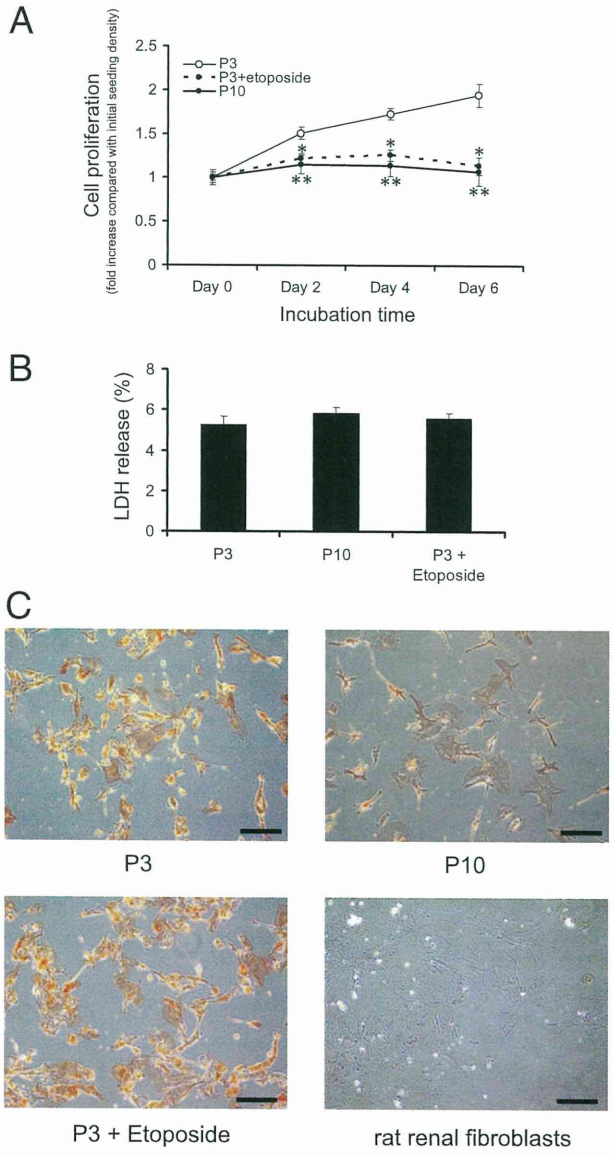

Figure 4. Validation of replicative senescence and senescence induced by etoposide in RPTECs. **A:** Cell proliferation rate determined by MTS assay showed replicative senescence at late passage (P10) and with exposure to a chemical senescence inducer, etoposide, at early passage (P3). Normal RPTECs doubled their population within 1 week, whereas senescent RPTECs and those exposed to etoposide did not proliferate. Assays were made at 2-day intervals, with the value on day 0 set as 1. $*P < 0.01$; $**P < 0.05$ versus day 0 of passage 3. **B:** LDH release was equivalent among RPTECs at passage 3 with or without etoposide exposure and at passage 10, excluding cells in which proliferation was halted because of cytotoxicity. LDH release = LDH in culture supernatant/(LDH in culture supernatant + LDH in cell lysate) ×100. **C:** Phase-contrast light micrographs with γ-GTP staining of RPTECs at passage 3 with or without etoposide exposure and at passage 10 and of rat renal fibroblasts confirmed that the cells retained the phenotype of proximal tubular cells. Original magnification = ×100. Scale bars: 200 μm. Red staining indicates cells positive for γ-GTP activity.

Of note, empty vector-transfected cells treated with etoposide showed a significant increase in SABG-positive cells, by 2.3 ± 1.0-fold, which was significantly suppressed by GLO1 overexpression (Figure 6, B and C). Transcript expression levels of p53, $p21^{WAF1/CIP1}$, and $p16^{INK4A}$, as well as protein expression levels of p53 in whole cellular lysate from etoposide-treated cells, were also significantly decreased in GLO1-transfected cells, compared with empty vector-transfected cells, whereas those without etoposide exposure showed no significant differences (Figure 6, D–F). Accumulation of CEL augmented by etoposide exposure was significantly suppressed by GLO1 overexpression, but remained at the increased levels with transfection of empty vector (Figure 6G).

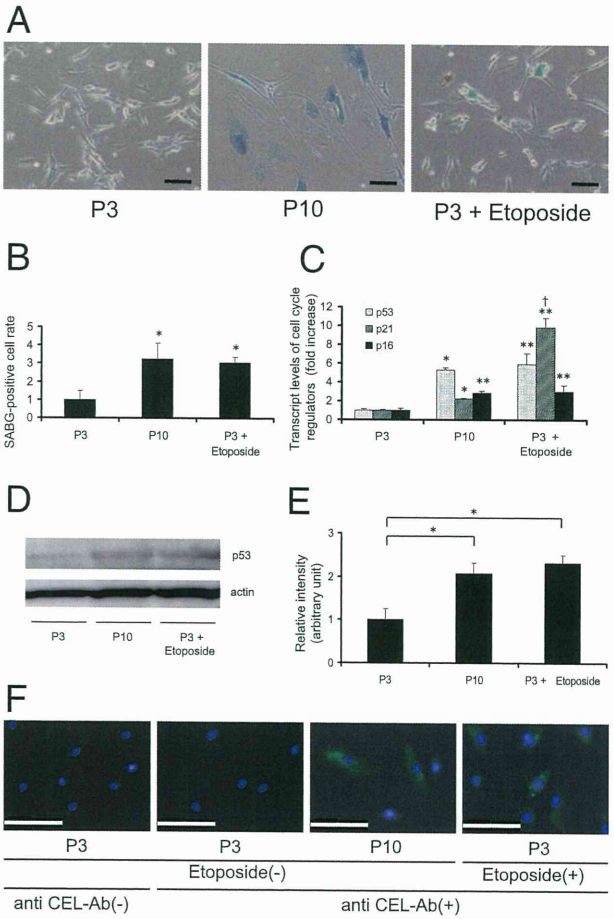

Figure 5. Carbonyl stress and cellular senescence in RPTECs. **A:** Phase-contrast light micrographs with SABG staining of RPTECs at passage 3 with or without etoposide exposure and at passage 10 show senescence of cells at passage 3 with etoposide exposure and at passage 10. Glutaraldehyde fixation was done before staining. SABG staining was performed by incubation for 5 hours without CO_2. Original magnification = ×100. Scale bars: 100 μm. Blue staining indicates positive cells. **B:** Quantitative analysis of SABG-positive cells per total cells in each field. Most RPTECs were senescent at passage 10 or with etoposide exposure. $*P < 0.01$ versus day 0 at passage 3. **C:** Transcript levels of p53, $p21^{WAF1/CIP1}$, and $p16^{INK4A}$ of RPTECs at passage 3 with or without etoposide exposure and at passage 10 determined by real-time quantitative RT-PCR. All showed significant elevation compared with cells at passage 3 without etoposide exposure. Values of those at passage 3 were set as 1. $*P < 0.01$; $**P < 0.05$ versus each at passage 3; $^{\dagger}P < 0.05$ versus $p21^{WAF1/CIP1}$ at passage 10. **D:** Protein immunoblot of p53 of whole lysate of RPTECs at passage 3 with or without etoposide exposure and at passage 10 confirmed the results of real-time quantitative PCR analysis. Cells were lysed in urea buffer under reducing conditions. Actin served as a control. **E:** Densitometric quantification of p53 immunoblot of RPTECs at early passage (P3) with or without etoposide exposure and at late passage (P10). The level of cells at early passage without etoposide exposure was set as 1. $*P < 0.01$ versus cells at passage 3 without etoposide exposure. **F:** Immunofluorescent micrographs for the detection of CEL showed carbonyl stress in senescent RPTECs. Only cells at passage 3 with etoposide exposure and at passage 10 exhibited a cytosolic positive signal. Cells were fixed with methanol 50%:acetone 50%. Green indicates anti-CEL (fluorescein isothiocyanate); blue stain identifies nuclei (Hoechst 33258 dye). Original magnification = ×400. Scale bars: 100 μm.

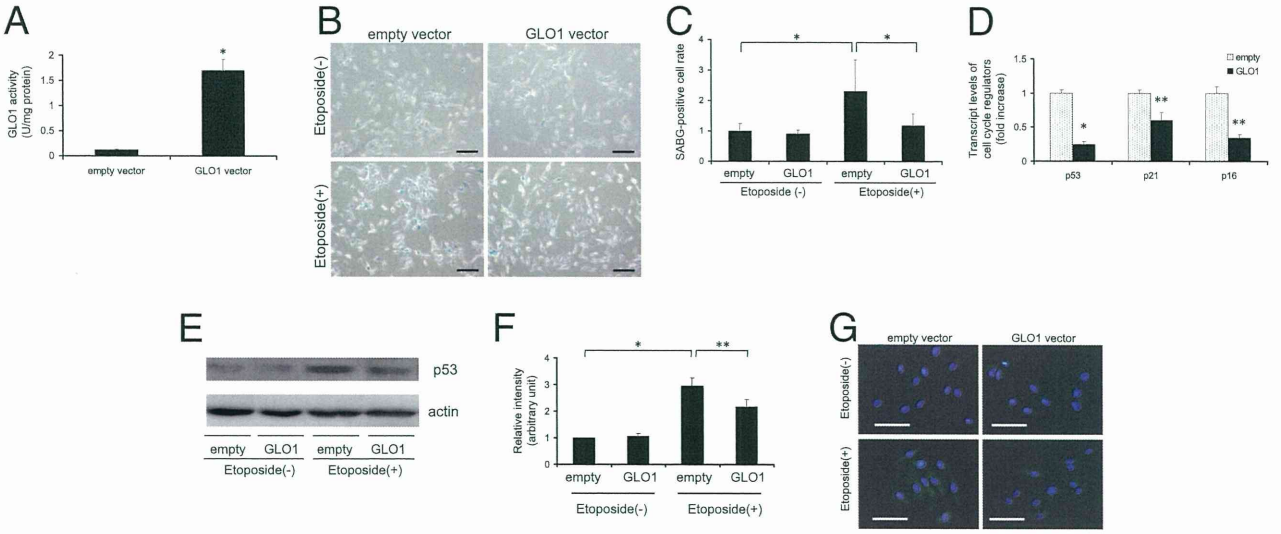

Figure 6. Attenuation of the senescent phenotypes of RPTECs at early passage with etoposide exposure by overexpression of GLO1. **A:** GLO1 activity assay measured at 24 hours after transfection of each vector confirmed successful overexpression of the transgene. Cells were lysed with sodium phosphate buffer with 1% Triton X-100 surfactant. $^{*}P < 0.01$ versus empty vector. **B:** Phase-contrast light micrographs with SABG staining of RPTECs at passages 3 to 4 transfected with empty vector or GLO1-containing vector with or without etoposide exposure showed amelioration of senescence by GLO1. Original magnification = ×100. Scale bars: 200 μm. Blue stain indicates SABG-positive cells. **C:** Quantitative analysis of SABG-positive cells per total cells in each field. $^{*}P < 0.01$ versus cells without etoposide exposure and transfected with empty vector. **D:** Relative transcript levels of p53, $p21^{WAF1/CIP1}$, and $p16^{INK4A}$ of RPTECs with etoposide exposure and transfected with plasmid vector determined by real-time quantitative RT-PCR. All showed a significant decrease in GLO1 transfectants, which demonstrated that GLO1 protected RPTECs against cellular senescence. Values of those transfected with empty vector were set as 1. $^{*}P < 0.01$; $^{**}P < 0.05$ versus cells transfected with empty vector. **E:** Protein immunoblot of p53 of whole lysate of RPTECs with or without etoposide exposure and transfected with plasmid vectors. p53 level in cells treated with etoposide exposure was ameliorated by GLO1 introduction. Actin serves as a control. **F:** Densitometric quantification of p53 immunoblot of RPTECs with or without etoposide exposure and transfected with plasmid vectors. The level of those transfected with empty vector without etoposide exposure was set as 1. $^{*}P < 0.01$; $^{**}P < 0.05$ versus cells without etoposide exposure and transfected with empty vector. **G:** Immunofluorescent micrographs of RPTECs with or without etoposide exposure and transfected with plasmid vectors for the detection of CEL accumulation. Cytosolic positive signals in cells exposed to etoposide were decreased by GLO1 introduction, demonstrating that overexpression of GLO1 ameliorated carbonyl stress. Green indicates anti-CEL (fluorescein isothiocyanate); blue stain identifies nuclei (Hoechst 33258 dye). Original magnification = ×400. Scale bars: 100 μm.

We also performed loss-of-function experiments with siRNA targeted to human GLO1 using two independent siRNAs against GLO1, which efficiently knocked down GLO1 expression and activity (Figure 7, A and B). Of note, when GLO1-knocked down cells were treated with etoposide, the number of cells positive for SABG staining was significantly increased, compared with control siRNA-transfected cells (Figure 7, C and D). Other senescence markers, such as transcript expression level of p53, $p21^{WAF1/CIP1}$, and $p16^{INK4A}$ or protein expression level of p53 in whole cellular lysate, were also markedly augmented by knockdown of GLO1 (Figure 7, E–G).

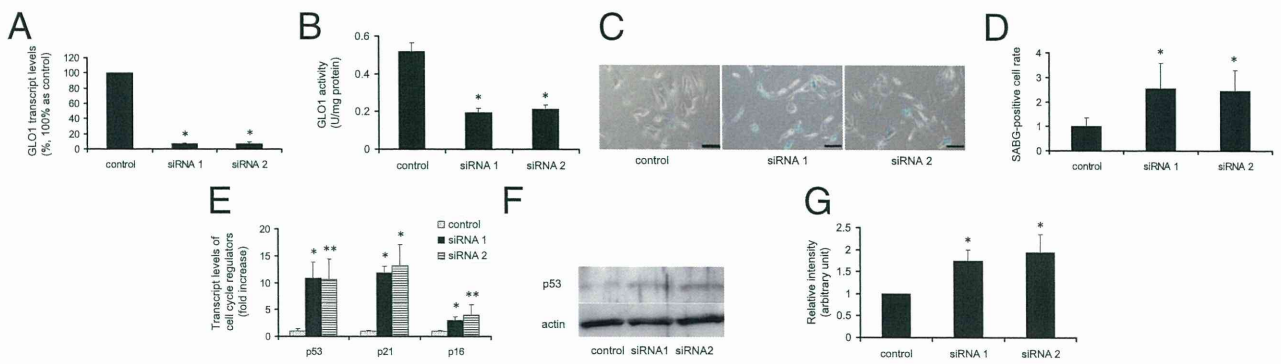

Figure 7. Knockdown of GLO1 exacerbated the senescence phenotype of RPTECs at early passage with etoposide exposure. **A:** Knockdown of the target gene was confirmed by transcript levels of GLO1 determined by real-time quantitative RT-PCR after 24 hours of transfection. The level of RPTECs transfected with control siRNA was set as 1. $^{*}P < 0.01$ versus control siRNA. **B:** GLO1 activity assay measured after 24 hours transfection with siRNA or control RNA was consistent with the decreased transcript levels. $^{*}P < 0.01$ versus empty vector. **C:** Phase-contrast light micrographs with SABG staining of RPTECs transfected with siRNA or control RNA with etoposide exposure showed aggravation of senescence by knockdown of GLO1. Original magnification = ×100. Scale bars: 100 μm. Blue stain indicates SABG-positive cells. **D:** Quantitative analysis of SABG-positive cells per total cells in each field. $^{*}P < 0.05$ versus cells with etoposide exposure and transfected with control siRNA. **E:** Relative transcript levels of p53, $p21^{WAF1/CIP1}$, and $p16^{INK4A}$ of RPTECs with etoposide exposure and transfected with siRNA or control RNA determined by real-time quantitative RT-PCR showed that knockdown of GLO1 aggravated cellular senescence phenotypes. Values of those transfected with control siRNA were set as 1. $^{*}P < 0.01$; $^{**}P < 0.05$ versus cells with etoposide exposure and transfected with control siRNA. **F:** Protein immunoblot of p53 of whole lysate of RPTECs with etoposide exposure and transfected with siRNA or control RNA. The level of p53 from cells exposed to etoposide was aggravated by the knockdown of GLO1. Actin serves as a control. **G:** Densitometric quantification of p53 immunoblot. The level of cells transfected with control siRNA was set as 1. $^{*}P < 0.05$ versus cells transfected with control siRNA.

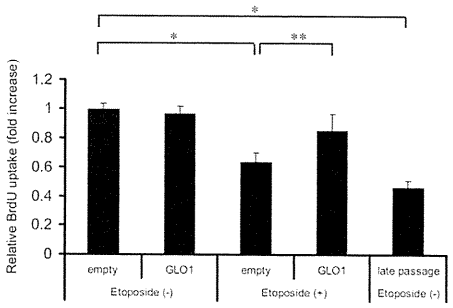

Figure 8. The replicative senescence induced by etoposide exposure was attenuated by transfection with the GLO1-overexpressing vector. BrdU uptake of RPTECs at early passage with or without etoposide exposure and at late passage without etoposide exposure was measured. BrdU uptake was significantly decreased by the addition of etoposide or at late passage, whereas the introduction of GLO1 ameliorated this decrease significantly. The level after transfection with empty vector without etoposide exposure was set as 1. $^{*}P < 0.01$; $^{**}P < 0.05$.

These gain-of-function and loss-of-function studies of GLO1 in cultured cells suggest that GLO1 has a cytoprotective effect against senescence.

Next, we verified the phenomena observed in the study of premature senescence by examining the status of replicative senescence on treatment with etoposide. Etoposide induced a significantly lower uptake of BrdU in RPTECs with mock transfection, and the degree of inhibition of BrdU uptake by etoposide was equivalent to that of late-passaged RPTECs (Figure 8). In contrast, cells overexpressing GLO1 showed no significant etoposide-induced decrease in the uptake of BrdU. These data demonstrate that the senescence status induced by etoposide, in which growth was inhibited and senescence markers were up-regulated, was ameliorated by GLO1.

Confirmation of Decrease in Renal Function of the Elderly Human Subjects with GLO1 Mutation

We had previously performed a nationwide analysis of GLO1 genotypes in schizophrenia patients and found that a minor subset of patients had frameshift mutations in GLO1.[24] Severe and significant decrease in the enzymatic activity was observed in those with frameshift mutations (3.0 ± 0.2 mU/10^6 red blood cells; $n = 3$), compared with WT GLO1 (6.8 ± 0.9 mU/10^6 red blood cells; $n = 244$). We investigated the effect of GLO1 activity on renal function. In the very rare cases with frameshift mutations, patients were all at the age of 50 to 60 years. We therefore compared the patients at this age, because GFR decreases with age.

Age-matched patients with WT GLO1 ($n = 15$) and frameshift mutation ($n = 3$) were analyzed. No clinically significant hematuria or proteinuria was found in any of the patients, with or without mutation. Neither musculature (determined by body mass index) nor systolic blood pressure, which could affect the serum creatinine levels, were significantly different among the three groups (Table 2). None of the patients with or without frameshift mutations were being treated with medication

Table 2. Physiological Characteristics of Elderly Schizophrenia Patients with or without *GLO1* Mutation

Characteristics	*GLO1* genotype	
	WT ($n = 15$)	Frameshift ($n = 3$)
Age (years)	56 ± 2.7	57 ± 4.6
Body mass index	23 ± 2.5	23 ± 4.9
Systolic blood pressure (mmHg)	110 ± 14	110 ± 11

No significant differences were observed in mean age, body mass index, or systolic blood pressure.

that could deteriorate renal functions. We reconfirmed a decreased activity of GLO1 in the patients with frameshift mutation, compared with the wild type (Figure 9A). Analysis of eGFR of the aged schizophrenia patients who had GLO1 frameshift mutations revealed significantly decreased renal function, compared with the wild type ($P < 0.01$) (Figure 9B). The data confirmed the protective effect of GLO1 against an age-dependent decrease in renal function.

Discussion

We found that the aged kidney shows an increase in AGE accumulation in association with a decrease in GLO1 activity, as is seen also in the aged human lens,[26] aged human red blood cells,[21] and aged human brain.[27,28] Thus, age-dependent acceleration of carbonyl stress may induce renal senescence, at least in part. Accordingly, GLO1 might reduce the senescence phenotype via inhibitory activity against carbonyl stress.[9] In the present study, we have demonstrated for the first time both *in vitro*

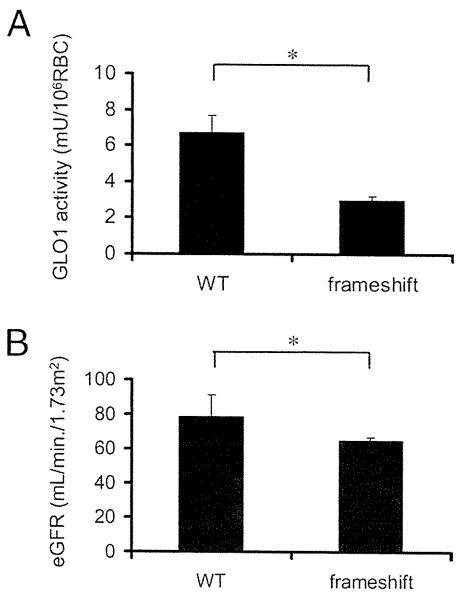

Figure 9. Analysis of human subjects with or without GLO mutations. **A:** GLO1 activity of red blood cells between the age-matched subjects with WT GLO1 and those with frameshift mutations of GLO1. WT, $n = 15$; frameshift, $n = 3$. $^{*}P < 0.01$. **B:** eGFR between age-matched subjects with WT GLO1 and those with frameshift mutations of GLO1. WT, $n = 15$; frameshift, $n = 3$. $^{*}P < 0.01$.

and *in vivo* that overexpression of GLO1 ameliorates all phenotypes of renal senescence. The delay in renal senescence in rats overexpressing GLO1 was associated with the preservation of kidney function. Furthermore, knockdown of GLO1 aggravated senescent phenotypes *in vitro*. Supporting a protective role of GLO1 against senescence, a recent report showed that overexpression of the GLO1 homolog CeGly induced longevity in *Caenorhabditis elegans*.[29]

We used 14-month-old rats for the aged group because we observed obvious histological changes associated with senescence in kidney in our preliminary experiments, as reported previously.[30] Because the aging process is complex and is likely to involve various mechanisms at different ages, we decided to focus on early senescence.

We focused our studies of kidney senescence on tubular epithelial cells. Functional impairment of the kidney more closely correlates with the degree of tubulointerstitial damage than with that of glomerular injury, and age-related decrease of eGFR is reported to be independent of glomerular change.[31] Our approach is consistent with several recent studies that have focused on tubulointerstitial alterations in the aging kidney.[30,32,33] One reason for the propensity toward senescence in the tubulointerstitium may relate to the metabolic rates of cells, given that podocytes or endothelial cells have far fewer mitochondria than tubular epithelial cells.[34]

In examination of a human specimen obtained from renal biopsy, we identified interstitial thickening (characterized by augmentation of matrix between tubules) as one of the senescent phenotypes of kidney. This alteration of renal components is distinct from interstitial fibrosis. Interstitial fibrosis is characterized by the replacement of tubules to fibrotic components and is observed in only limited portions of kidney, whereas interstitial thickening is a generalized change in the kidney. More importantly, this age-related phenotype is observed across a wide range of ages; in contrast, thickness of glomerular basement membrane is reported to have different effects at different ages.[35] To prevent overestimation of the interstitial thickness for tubules at an angle to the cutting surface, we measured the smallest thickness around tubules.

In the present study, RPTECs reached replicative senescence status at 10 passages, which is earlier than for primary cultured fibroblasts, which do so at approximately 40 passages. This finding is consistent with a previous report,[36] and might reflect high metabolic rate, susceptibility to senescence, or the nature of high differentiation. We also used etoposide, a well-established chemical senescence inducer,[37–40] to induce the cultured cells into senescence. The senescent phenotypes induced by etoposide were equivalent to those observed in late-passaged cells (although we note that the mechanism by which etoposide induces senescence has not been clarified).

The expression of senescence markers such as SABG, $p16^{INK4A}$, $p21^{WAF1/CIP1}$, and p53 was significantly increased in both late-passaged primary tubular epithelial cells and in the tubules of aged rat kidneys. Staining for p53 was positive not only in the nuclei but also in the cytoplasm, as reported previously.[41,42] These senescent phenotypes were associated *in vivo* with interstitial thickening in both human and rat kidney. Interstitial thickening might represent an aging-specific morphological change at an early stage of kidney aging. Similar changes were observed in a rodent model that was enhanced to present an age-related phenotype.[43,44]

Our analysis of schizophrenia patients demonstrated association of reduction of GLO1 activity and accelerated age-dependent deterioration of renal function in human. Age-dependent decline of renal function in subjects with preserved GLO1 activity was consistent with that described in healthy aged individuals previously (0.64 to 0.75 mL/min per year).[45–47] These results suggest that the difference in deterioration of age-dependent renal function that we observed was not due to improvement of renal function in schizophrenia patients with preserved GLO1 activity but rather was due to acceleration of age-dependent renal dysfunction associated with decreased GLO1 activity. One limitation is that these data are based on a small number of subjects in the GLO1-mutated group ($n = 3$); however, the incidence rate of this mutation is so low that this difficulty cannot be avoided.

Although excessive carbonyl stress is considered to be a major cause of spontaneous damage to intracellular and extracellular proteins functions,[48] detailed mechanisms of the progression of senescence by carbonyl stress remain to be elucidated.

In conclusion, we have established a role of carbonyl stress in senescence and demonstrated that GLO1 can retard renal senescence both *in vitro* and *in vivo*.

References

1. Dimri GP, Lee X, Basile G, Acosta M, Scott G, Roskelley C, Medrano EE, Linskens M, Rubelj I, Pereira-Smith O, Peacocke M, Campisi J: A biomarker that identifies senescent human cells in culture and in aging skin in vivo. Proc Natl Acad Sci USA 1995, 92:9363–9367
2. Duncan EL, Wadhwa R, Kaul SC: Senescence and immortalization of human cells. Biogerontology 2000, 1:103–121
3. Collado M, Serrano M: The power and the promise of oncogene-induced senescence markers. Nat Rev Cancer 2006, 6:472–476
4. Harman D: Aging: a theory based on free radical and radiation chemistry. J Gerontol 1956, 11:298–300
5. Perez VI, Bokov A, Remmen HV, Mele J, Ran Q, Ikeno Y, Richardson A: Is the oxidative stress theory of aging dead? Biochim Biophys Acta 2009, 1790:1005–1014
6. Pérez VI, Van Remmen H, Bokov A, Epstein CJ, Vijg J, Richardson A: The overexpression of major antioxidant enzymes does not extend the lifespan of mice. Aging Cell 2009, 8:73–75
7. Stadtman ER: Protein oxidation and aging. Science 1992, 257:1220–1224
8. Thorpe SR, Baynes JW: Role of the Maillard reaction in diabetes mellitus and diseases of aging. Drugs Aging 1996, 9:69–77
9. Thornalley PJ: Protein and nucleotide damage by glyoxal and methylglyoxal in physiological systems: role in ageing and disease. Drug Metabol Drug Interact 2008, 23:125–150
10. Finkel T, Holbrook NJ: Oxidants, oxidative stress and the biology of ageing. Nature 2000, 408:239–247
11. Uribarri J, Cai W, Peppa M, Goodman S, Ferrucci L, Striker G, Vlassara H: Circulating glycotoxins and dietary advanced glycation endproducts: two links to inflammatory response, oxidative stress, and aging. J Gerontol A Biol Sci Med Sci 2007, 62:427–433
12. Münch G, Shepherd CE, McCann H, Brooks WS, Kwok JB, Arendt T, Hallupp M, Schofield PR, Martins RN, Halliday GM: Intraneuronal

advanced glycation endproducts in presenilin-1 Alzheimer's disease. Neuroreport 2002, 13:601–604
13. Ahmed N: Advanced glycation endproducts–role in pathology of diabetic complications. Diabetes Res Clin Pract 2005, 67:3–21
14. Chen J, Huang X, Halicka D, Brodsky S, Avram A, Eskander J, Bloomgarden NA, Darzynkiewicz Z, Goligorsky MS: Contribution of p16INK4a and p21CIP1 pathways to induction of premature senescence of human endothelial cells: permissive role of p53. Am J Physiol Heart Circ Physiol 2006, 290:H1575–H1586
15. Thangarajah H, Yao D, Chang EI, Shi Y, Jazayeri L, Vial IN, Galiano RD, Du XL, Grogan R, Galvez MG, Januszyk M, Brownlee M, Gurtner GC: The molecular basis for impaired hypoxia-induced VEGF expression in diabetic tissues. Proc Natl Acad Sci USA 2009, 106:13505–13510
16. Thornalley PJ: The glyoxalase system: new developments towards functional characterization of a metabolic pathway fundamental to biological life. Biochem J 1990, 269:1–11
17. Hayes JD, Milner SW, Walker SW: Expression of glyoxalase, glutathione peroxidase and glutathione S-transferase isoenzymes in different bovine tissues. Biochim Biophys Acta 1989, 994:21–29
18. Thornalley PJ: Glyoxalase I–structure, function and a critical role in the enzymatic defence against glycation. Biochem Soc Trans 2003, 31:1343–1348
19. Kumagai T, Nangaku M, Kojima I, Nagai R, Ingelfinger JR, Miyata T, Fujita T, Inagi R: Glyoxalase I overexpression ameliorates renal ischemia-reperfusion injury in rats. Am J Physiol Renal Physiol 2009, 296:F912–F921
20. Inagi R, Miyata T, Ueda Y, Yoshino A, Nangaku M, van Ypersele de Strihou C, Kurokawa K: Efficient in vitro lowering of carbonyl stress by the glyoxalase system in conventional glucose peritoneal dialysis fluid. Kidney Int 2002, 62:679–687
21. McLellan AC, Thornalley PJ: Glyoxalase activity in human red blood cells fractioned by age. Mech Ageing Dev 1989, 48:63–71
22. Nagai R, Fujiwara Y, Mera K, Yamagata K, Sakashita N, Takeya M: Immunochemical detection of Nepsilon-(carboxyethyl)lysine using a specific antibody. J Immunol Methods 2008, 332:112–120
23. Rutenburg AM, Kim H, Fischbein JW, Hanker JS, Wasserkrug HL, Seligman AM: Histochemical and ultrastructural demonstration of gamma-glutamyl transpeptidase activity. J Histochem Cytochem 1969, 17:517–526
24. Arai M, Yuzawa H, Nohara I, Ohnishi T, Obata N, Iwayama Y, Haga S, Toyota T, Ujike H, Arai M, Ichikawa T, Nishida A, Tanaka Y, Furukawa A, Aikawa Y, Kuroda O, Niizato K, Izawa R, Nakamura K, Mori N, Matsuzawa D, Hashimoto K, Iyo M, Sora I, Matsushita M, Okazaki Y, Yoshikawa T, Miyata T, Itokawa M: Enhanced carbonyl stress in a subpopulation of schizophrenia. Arch Gen Psychiatry 2010, 67:589–597
25. Matsuo S, Imai E, Horio M, Yasuda Y, Tomita K, Nitta K, Yamagata K, Tomino Y, Yokoyama H, Hishida A; Collaborators developing the Japanese equation for estimated GFR: Revised equations for estimated GFR from serum creatinine in Japan. Am J Kidney Dis 2009, 53:982–992
26. Haik GM Jr, Lo TW, Thornalley PJ: Methylglyoxal concentration and glyoxalase activities in the human lens. Exp Eye Res 1994, 59:497–500
27. Kuhla B, Boeck K, Lüth HJ, Schmidt A, Weigle B, Schmitz M, Ogunlade V, Münch G, Arendt T: Age-dependent changes of glyoxalase I expression in human brain. Neurobiol Aging 2006, 27:815–822
28. Kuhla B, Boeck K, Schmidt A, Ogunlade V, Arendt T, Münch G, Lüth HJ: Age- and stage-dependent glyoxalase I expression and its activity in normal and Alzheimer's disease brains. Neurobiol Aging 2007, 28:29–41
29. Morcos M, Du X, Pfisterer F, Hutter H, Sayed AA, Thornalley P, Ahmed N, Baynes J, Thorpe S, Kukudov G, Schlotterer A, Bozorgmehr F, El Baki RA, Stern D, Moehrlen F, Ibrahim Y, Oikonomou D, Hamann A, Becker C, Zeier M, Schwenger V, Miftari N, Humpert P, Hammes HP, Buechler M, Bierhaus A, Brownlee M, Nawroth PP: Glyoxalase-1 prevents mitochondrial protein modification and enhances lifespan in Caenorhabditis elegans. Aging Cell 2008, 7:260–269
30. Ding G, Franki N, Kapasi AA, Reddy K, Gibbons N, Singhal PC: Tubular cell senescence and expression of TGF-beta1 and p21(WAF1/CIP1) in tubulointerstitial fibrosis of aging rats. Exp Mol Pathol 2001, 70:43–53
31. Rule AD, Am H, Cornell LD, Taler SJ, Cosio FG, Kremers WK, Textor SC, Stegall MD: The association between age and nephrosclerosis on renal biopsy among healthy adults. Ann Intern Med 2010, 152:561–567
32. Abrass CK, Adcox MJ, Raugi GJ: Aging-associated changes in renal extracellular matrix. Am J Pathol 1995, 146:742–752
33. Ruiz-Torres MP, Bosch RJ, O'Valle F, Del Moral RG, Ramírez C, Masseroli M, Pérez-Caballero C, Iglesias MC, Rodríguez-Puyol M, Rodríguez-Puyol D: Age-related increase in expression of TGF-beta1 in the rat kidney: relationship to morphologic changes. J Am Soc Nephrol 1998, 9:782–791
34. Pease DC: Fine structures of the kidney seen by electron microscopy. J Histochem Cytochem 1955, 3:295–308
35. Shindo S, Yoshimoto M, Kuriya N, Bernstein J: Glomerular basement membrane thickness in recurrent and persistent hematuria and nephrotic syndrome: correlation with sex and age. Pediatr Nephrol 1988, 2:196–199
36. Glynne PA: Primary culture of human proximal renal tubular epithelial cells. Methods Mol Med 2000, 36:197–205
37. Krizhanovsky V, Yon M, Dickins RA, Hearn S, Simon J, Miething C, Yee H, Zender L, Lowe SW: Senescence of activated stellate cells limits liver fibrosis. Cell 2008, 134:657–667
38. te Poele RH, Okorokov AL, Jardine L, Cummings J, Joel SP: DNA damage is able to induce senescence in tumor cells in vitro and in vivo. Cancer Res 2002, 62:1876–1883
39. Robles SJ, Buehler PW, Negrusz A, Adami GR: Permanent cell cycle arrest in asynchronously proliferating normal human fibroblasts treated with doxorubicin or etoposide but not camptothecin. Biochem Pharmacol 1999, 58:675–685
40. Wang Y, Blandino G, Oren M, Givol D: Induced p53 expression in lung cancer cell line promotes cell senescence and differentially modifies the cytotoxicity of anti-cancer drugs. Oncogene 1998, 17:1923–1930
41. Kaserer K, Schmaus J, Bethge U, Migschitz B, Fasching S, Walch A, Herbst F, Teleky B, Wrba F: Staining patterns of p53 immunohistochemistry and their biological significance in colorectal cancer. J Pathol 2000, 190:450–456
42. Ranade KJ, Nerurkar AV, Phulpagar MD, Shirsat NV: Expression of survivin and p53 proteins and their correlation with hormone receptor status in Indian breast cancer patients. Indian J Med Sci 2009, 63:481–490
43. Samuel CS, Zhao C, Bond CP, Hewitson TD, Amento EP, Summers RJ: Relaxin-1-deficient mice develop an age-related progression of renal fibrosis. Kidney Int 2004, 65:2054–2064
44. Floege J, Hackmann B, Kliem V, Kriz W, Alpers CE, Johnson RJ, Kühn KW, Koch KM, Brunkhorst R: Age-related glomerulosclerosis and interstitial fibrosis in Milan normotensive rats: a podocyte disease. Kidney Int 1997, 51:230–243
45. Lindeman RD, Tobin J, Shock NW: Longitudinal studies on the rate of decline in renal function with age. J Am Geriatr Soc 1985, 33:278–285
46. Rowe JW, Andres R, Tobin JD: Letter: age-adjusted standards for creatinine clearance. Ann Intern Med 1976, 84:567–569
47. Rowe JW, Andres R, Tobin JD, Norris AH, Shock NW: The effect of age on creatinine clearance in men: a cross-sectional and longitudinal study. J Gerontol 1976, 31:155–163
48. Thornalley PJ, Battah S, Ahmed N, Karachalias N, Agalou S, Babaei-Jadidi R, Dawnay A: Quantitative screening of advanced glycation endproducts in cellular and extracellular proteins by tandem mass spectrometry. Biochem J 2003, 375:581–592

Psychiatry and Clinical Neurosciences 2011; 65: 604–607

of the Wechsler Intelligence Scale, third edition (WAIS-III), his full-scale intelligence quotient (IQ) was 124, verbal IQ was 130, and performance IQ was 112. Marked deviations were seen in some subtests of the WAIS-III, with very high performance in Vocabulary and Information, and very low performance in Letter–number sequencing and Picture completion. Magnetic resonance imaging (MRI) of the head and encephalography yielded results within normal limits. These findings suggested autistic disorder (high-functioning autism) according to DSM-IV-TR criteria.

Collagens represent a large family of structurally related extracellular matrix proteins essential for development, cell attachment, platelet aggregation and tensile strength in connective tissues such as bone, skin, ligaments, tendons, and blood vessels.[3] Cupo *et al.* described abnormalities in the development of the central nervous system (CNS) in EDS, including a heterotropic formation in the CNS.[4] Although no CNS abnormality was evident on MRI in the present case, loss of elasticity and strength of collagen presumably contributed to structural failure in connective tissues of the CNS. We speculate that associations exist between connective tissue diseases and autistic disorders, and that connective tissue abnormalities may contribute to autistic symptoms.

REFERENCES

1. Tantam D, Evered C, Hersov L. Asperger's syndrome and ligamentous laxity. *J. Am. Acad. Child Adolesc. Psychiatry* 1990; 29: 892–896.
2. Sieg KG. Autism and Ehlers-Danlos syndrome. *J. Am. Acad. Child Adolesc. Psychiatry* 1992; 31: 173.
3. De Paepe A, Malfait F. Bleeding and bruising in patients with Ehlers-Danlos syndrome and other collagen vascular disorders. *Br. J. Haematol.* 2004; 127: 491–500.
4. Cupo LN, Pyeretz R, Olson J, McPhee S, Hutchins G, McKusick V. Ehlers-Danlos syndrome with abnormal collagen fibrils, sinus of Valsalva aneurysms, myocardial infraction, panacinar emphysema and cerebral heterotopics. *Am. J. Med.* 1981; 71: 1051–1058.

Akira Takei, MD, Kazuhiko Mera, MD, Yuzuru Sato, MD and Yoichi Haraoka, MD
Department of Psychiatry, Asahikawa City Hospital, Asahikawa, Japan
Email: a_takei@city.asahikawa.hokkaido.jp
Received 20 April 2011; revised 21 June 2011; accepted 8 August 2011.

Idiopathic carbonyl stress in a drug-naive case of at-risk mental state

doi:10.1111/j.1440-1819.2011.02261.x

WE PREVIOUSLY REPORTED that a subgroup of schizophrenia patients exhibit carbonyl stress with high plasma pentosidine levels, without underlying diabetes mellitus or chronic kidney disease, the two major causes of elevated, advanced glycation end-products.[1] These patients, however, had previously received antipsychotic therapy, leaving the possible role of medication in carbonyl stress unclear. Here, we report on a drug-naive patient with at-risk mental state (ARMS), who exhibited enhanced carbonyl stress with high plasma pentosidine levels.

The patient was a 21-year-old male college student, who was born at full term after an uneventful pregnancy and delivery. He first developed obsessive thoughts at age 18 and sought medical help because of communication difficulties and depression. He was diagnosed with obsessive and compulsive disorder (OCD) according to DSM-IV criteria. Biweekly counseling and psychotherapy temporarily reduced his symptoms but a persistence of confused thoughts, hearing hypersensitivity and delusional ideation of persecution and reference led to a diagnosis of ARMS, according to Structured Interview for Prodromal Syndromes (SIPS) criteria, 10 months after his initial consultation. He was followed clinically for 12 months and treated temporarily with 0.5 mg of etizolam and 5 mg of zolpidem, which improved his symptoms. He entered a research study on ARMS and his symptoms were scaled and biochemical data measured at his initial visit, and also after 16 months of treatment. During this period his score on the Positive and Negative Syndrome Scale decreased from 84 to 58 ($P = 0.001$), his positive subscale score changed from 20 to 22 ($P = 0.38$), negative subscale score changed from 22 to 9 ($P = 0.03$) and the general psychopathology subscale score changed from 42 to 27 ($P = 0.008$). Global Assessment of Functioning also improved from 55 to 65. Plasma pentosidine levels decreased from 113.2 to 44.1 ng/mL. We did not measure carbonyl compounds such as methylglyoxal (MG), carbohydrate precursors of pentosidine and advanced glycation adducts: $N(\varepsilon)$-(carboxymethyl)lysine and $N(\varepsilon)$-(carboxyethyl)lysine. We did not assess the activity of glyoxalase1 (GLO1) or pyridoxal levels before treatment, but after treatment the activity was 7.55 mU/10^6 red blood cells, and the pyridoxal level was 6.8 ng/mL, and these are both normal levels for the enzyme and pyridoxal, respectively. It is not known whether etizolam and zolpidem affect pentosidine levels. In the preliminary data, the dose (mg/day) of etizolam ($n = 18$) or zolpidem ($n = 11$) was not significantly correlated with pentosidine levels in patients with schizophrenia (data not shown). The patients were also taking other drugs, however, and thus the lack of apparent correlation is not conclusive. The GLO1 genotype in the present case was wild type (c.332A>C, p.Glu111/Glu111). Biochemistry did not demonstrate any abnormalities indicative of disease, such as diabetes mellitus or chronic kidney diseases.

The present case report does not demonstrate a direct link between carbonyl stress and the disease development. It is not known whether carbonyl stress is a cause or consequence of the disease. In addition, it cannot be ruled out that other physical conditions or drugs affected the pentosidine levels. Additional data are needed to clarify a possible relationship between carbonyl stress and mental disorders.

The ethics committees for the University of Tokyo and Tokyo Institute of Medical Science approved the present study (2089-(2), 2094-(2), 2226-(1), 21–2). The subject gave written informed consent in accordance with the Declaration of Helsinki after a complete explanation of the original study. After

ethics approval, the patient re-consented for publication of this case report.

This study was supported by grants from the Ministry of Health, Labour, and Welfare (H22-seishin-ippan-015 to KK), and from the JSPS/MEXT (No. 21249064 and Grant-in-Aid for Scientific Research on Innovative Areas [Comprehensive Brain Science Network] to KK, No. 20249054 and Grant-in-Aid for Scientific Research (A), no. 22129007 and Grant-in-Aid for Scientific Research on Priority Areas to MI). A part of this study was also the result of 'Development of biomarker candidates for social behavior' carried out under the Strategic Research Program for Brain Sciences by MEXT.

REFERENCE

1. Arai M, Yuzawa H, Nohara I *et al.* Enhanced carbonyl stress in a subpopulation of schizophrenia. *Arch. Gen. Psychiatry* 2010; 67: 589–597.

Makoto Arai, PhD,[1] Shinsuke Koike, MD,[2] Norihito Oshima, MD,[3] Ryu Takizawa, MD,[2] Tsuyoshi Araki, MD, PhD,[2] Mitsuhiro Miyashita, MD,[1] Atsushi Nishida, PhD,[1] Toshio Miyata, MD, PhD,[4] Kiyoto Kasai, MD, PhD[2] and Masanari Itokawa, MD, PhD[1]

[1]*Project for Schizophrenia and Affective Disorders Research, Tokyo Metropolitan Institute of Medical Science,* [2]*Department of Neuropsychiatry, Graduate School of Medicine,* [3]*Division for Counseling and Support, Office for Mental Health Support, University of Tokyo, Tokyo, and* [4]*Center for Translational and Advanced Research on Human Disease, Tohoku University Graduate School of Medicine, Miyagi, Japan*

Email: itokawa-ms@igakuken.or.jp

Received 27 April 2011; revised 7 July 2011; accepted 8 August 2011.

Aripiprazole monotherapy in the treatment of vascular parkinsonism

doi:10.1111/j.1440-1819.2011.02263.x

VASCULAR PARKINSONISM (VP) is characterized by poor response to levodopa. In contrast, reduced presynaptic dopaminergic activity, the main pathology of Parkinson's disease (PD), is not suggested in VP.[1] Dopamine D2 partial agonists have been suggested as a potential therapeutic approach to the treatment of the motor symptoms of PD that may avoid common dopaminergic side-effects including dyskinesia and psychosis.[2] We report a first case of antiparkinsonian agent-refractory VP in which both psychosis and parkinsonism were treated successfully using aripiprazole monotherapy.

A 75-year-old woman with an 8-year history of antiparkinsonian agent-refractory VP was admitted to Department of Neuropsychiatry, Fukui University Hospital for treatment for psychosis. On admission, treatment consisted of 400 mg/day of L-dopa/carbidopa, 100 mg/day of droxidopa, and 100 mg/day of amantadine. The patient had showed postural tremor, gait disorder, and pyramidal signs with lower-body predominance and mild cognitive impairment (Mini-Mental State Examination: 22/30). The severity score on the Unified Parkinson's Disease Rating Scale (UPDRS) was 118. The illness stage according to the Hoehn and Yahr scale was IV. The patient exhibited frank psychosis with vivid visual hallucinations and fearful delusions of persecution (severity score on the Brief Psychiatric Rating Scale [BPRS] was 96). Results of laboratory tests, electrocardiography, and electroencephalography were normal. Myocardial ^{123}I-metaiodobenzylguanidine indicated a normal heart to mediastinum ratio; cranial magnetic resonance imaging showed multiple deep subcortical lesions. Antiparkinsonian medications were gradually tapered off with no apparent clinical changes of parkinsonism. Her psychotic symptoms improved to a large extent (BPRS score, 52) on day 20, but visual hallucinations persisted. On day 34, aripiprazole monotherapy was started at 3 mg/day and increased by 3 mg every week up to 9 mg. Her psychosis gradually improved (BPRS score, 32), with dramatic amelioration of parkinsonism (UPDRS score, 43), especially in activities of daily living and motor examination items of UPDRS. Using the same regimen, no worsening of psychiatric or neurological symptoms had occurred 7 months after discharge.

In the present case, aripiprazole improved pharmacologically paradoxical symptoms such as psychosis and parkinsonism by the stabilization of dopaminergic activity through dopamine D2 partial agonistic properties.[3] Cerebrovascular lesions, which are suggested as a mechanism for VP,[1] might cause not reduced presynaptic dopaminergic activity but dysregulated dopaminergic activity. Although the utility of aripiprazole in managing psychosis and parkinsonism in PD remains controversial,[4,5] the present case suggests the potential utility of aripiprazole monotherapy in treating VP.

REFERENCES

1. Kalra S, Grosset DG, Benamer HT. Differentiating vascular parkinsonism from idiopathic Parkinson's disease: A systematic review. *Mov. Disord.* 2010; 25: 149–156.
2. Bronzova J, Sampaio C, Hauser RA *et al.* Double-blind study of pardoprunox, a new partial dopamine agonist, in early Parkinson's disease. *Mov. Disord.* 2010; 25: 730–738.
3. Jordan S, Koprivica V, Dunn R, Tottori K, Kikuchi T, Altar CA. In vivo effects of aripiprazole on cortical and striatal dopaminergic and serotonergic function. *Eur. J. Pharmacol.* 2004; 483: 45–53.
4. Fernandez HH, Trieschmann ME, Friedman JH. Aripiprazole for drug-induced psychosis in Parkinson disease: Preliminary experience. *Clin. Neuropharmacol.* 2004; 27: 4–5.
5. Fujino J, Tanaka H, Taniguchi N, Tabushi K. Effectiveness of aripiprazole in a patient with presumed idiopathic Parkinson's disease and chronic paranoid schizophrenia. *Psychiatry Clin. Neurosci.* 2010; 64: 108–109.

Makoto Ishitobi, MD, PhD, Hirotaka Kosaka, MD, PhD, Tetsuya Takahashi, MD, PhD, Makiyo Oonuma, MD, Tetsuhito Murata, MD, PhD and Yuji Wada, MD, PhD

Department of Neuropsychiatry, University of Fukui, Fukui, Japan

Email: mak1977019@yahoo.co.jp

Received 21 June 2011; revised 29 July 2011; accepted 8 August 2011.

BJPsych | The British Journal of Psychiatry (2011) 199, 245–246. doi: 10.1192/bjp.bp.111.093849

Short report

Schizophrenia with the 22q11.2 deletion and additional genetic defects: case history

M. Toyosima,* M. Maekawa,* T. Toyota, Y. Iwayama, M. Arai, T. Ichikawa, M. Miyashita, T. Arinami, M. Itokawa and T. Yoshikawa

Summary

The 22q11.2 deletion is the most prominent known genetic risk factor for schizophrenia, but its penetrance is at most approximately 50% suggesting that additional risk factors are required for disease progression. We examined a woman with schizophrenia with this deletion for such risk factors. She had high plasma pentosidine levels ('carbonyl stress') and a frameshift mutation in the responsible gene, *GLO1*. She also had a constant exotropia, so we examined the *PHOX2B* gene associated with both schizophrenia and strabismus, and detected a 5-alanine deletion. We propose that the combination of these genetic defects may have exceeded the threshold for the manifestation of schizophrenia.

Declaration of interest

None.

Schizophrenia is a debilitating and relatively common mental illness, with a prevalence of approximately 1% worldwide. Although the exact aetiology is unknown, the genetic pathology is thought to consist of numerous weak, risk-conferring genomic variations and/or rare, large-effect variations. An example of the latter is copy number variants (CNVs), typified by the 22q11.2 deletion syndrome (22q11.2DS; also known as the velocardiofacial syndrome or DiGeorge syndrome)[1] caused by a microdeletion (1.5–3 Mb) of chromosome 22, with an incidence of 1 in 2000–4000 live births. The phenotype of this disorder is highly variable and common physical manifestations include craniofacial and cardiovascular anomalies, immunodeficiency, short stature and hypocalcaemia. In late adolescence and early adulthood, up to 50% of all individuals with 22q11.2DS develop schizophrenia or schizoaffective disorder.[1] The 22q11.2 deletion is therefore one of the greatest known genetic risk factors for schizophrenia. However, penetrance is incomplete and the remaining 22q11.2DS carriers do not develop disease. We asked whether combinations of additional genomic flaws may be needed to develop schizophrenia and here we describe an individual with 22q11.2DS with schizophrenia, and in whom we detected two additional rare schizophrenia-associated genetic defects. The individual's written consent to publish was obtained.

Method

Previously, we screened 300 unrelated Japanese individuals with schizophrenia who met the DSM-III-R[2] diagnostic criteria for schizophrenia, by genotyping of markers D22S941, D22S944, D22S264 and D22S311.[3] Concomitantly, we detected one patient with only one allele for each of these polymorphic markers. This individual was a female high-school graduate then aged 28 years. She was born by normal delivery without any obstetric complications. She was admitted to hospital at the age of 18 years for 2 months and again at the age of 25 years for 1 month. Her IQ, which was measured during her first hospital admission, was 61. We decided to re-evaluate her in August 2010. At this time, she was 37 years old and being treated with antipsychotics (risperidone 5 mg/day and quetiapine 95 mg/day), but still suffered from persistent auditory hallucinations. Her only physical symptom was a slight hypocalcaemia (8.4 mg/dl in serum, normal range 8.5–10.5 mg/dl). She remains unmarried, lives in a group home and is employed in a semi-sheltered workplace. We re-examined her 22q11.2 microdeletion by fluorescence *in situ* hybridisation (FISH) with the TUBLE1 probe, and using the NimbleGen Human CNV 3x720K v1.0 Array (Roche Applied Science, Tokyo, Japan).

We recently reported that a subpopulation of individuals with schizophrenia have high plasma pentosidine levels (i.e. 'carbonyl stress') and in 2 such individuals out of 3682 participants, we detected frameshift mutations (P122LfsX27 and T27NfsX15) in the glyoxalase I (*GLO1*) gene, a zinc metalloenzyme, providing a possible explanation for the high plasma pentosidine levels.[4] Therefore, we set out to measure pentosidine levels in our patient by high-performance liquid chromatography assay and perform a re-sequencing analysis of *GLO1*, as described previously.[4]

In another previous report, we showed an association between polyalanine stretch length polymorphisms of the paired-like homeobox 2b (*PMX2B* or *PHOX2B*) gene encoding a transcription factor, with people who have schizophrenia, in particular those with strabismus.[5] As our patient has constant exotropia in her right eye, we examined this gene: briefly, the genomic region encoding the 20-alanine tract was amplified using fluorescently labelled forward and reverse primers. Polymerase chain reaction products were run on an ABI 3130xl genetic analyser and the resulting data analysed using the Gene Mapper and Peak Scanner software (Applied Biosystems, Foster City, California, USA).

Results

The FISH data (online Fig. DS1(a)) and the microarray-based CNV analysis (not shown) revealed that the woman has a 3 Mb hemizygous genomic deletion on chromosome 22q11.2, confirming that she has 22q11.2DS. An echocardiogram examination showed no abnormalities in the cardiovascular system (online Fig. DS2). We measured her plasma pentosidine levels twice, 1 week apart, and both values exceeded the mean +2 standard deviation levels of healthy controls ($n=61$)[4] (online Fig. DS1(b)). Then, we examined the *GLO1* gene and identified a frameshift mutation

*These two authors contributed equally to this work.

(P122LfsX27; identical to one of our previously detected mutations[4]) (online Fig. DS1(c)). An examination of the *PHOX2B* gene revealed a 5-alanine deletion within the 20-alanine stretch region (online Fig. DS1(d)).

Discussion

The frequencies of schizophrenia-associated CNVs are rare but generally have larger effects on susceptibility to the disease compared with risk-conferring single nucleotide polymorphisms. Among such CNVs, the 22q11.2 deletion has the deepest penetrance of 0.553 (95% CI 0.18–0.97).[6] The penetrance of other large effect size CNVs, for example the 15q13.3 deletion and 16p11.2 duplication are 0.074 (95% CI 0.03–0.16) and 0.069 (95% CI 0.03–0.14) respectively.[6] Nonetheless, the 22q11.2 deletion is not sufficient to develop schizophrenia, and other risk factors are required. This case demonstrates for the first time to our knowledge that concrete additional risk variants could contribute to the manifestation of schizophrenia in combination with 22q11.2DS. In view of the penetrance of these mutations, this view has to be a qualified one as other causative mutations may contribute to this individual's developmental phenotypes.

We show that one contributing factor is the accumulation of pentosidine, an advanced glycation end-product resulting from carbonyl stress, a state featuring an increase in reactive carbonyl compounds and their attendant protein modifications. Our prior study demonstrated that people with schizophrenia have significantly higher plasma pentosidine levels than controls, and revealed that some participants with high pentosidine levels have impaired GLO1 activity, which is caused by a Glu111→Ala amino acid change and frameshift mutations (see below).[4] Cellular removal of reactive carbonyl compounds, including pentosidine, hinges largely on the activity of GLO1.[7] The identified frameshift mutations were P122LfsX27 and T27NfsX15 (one each out of 1761 participants with schizophrenia), both of which elicit nonsense-mediated mRNA decay resulting in a reduction (to 40–50%) of GLO1 protein expression and activity.[4] The current patient carries the P122LfsX27 frameshift mutation, coincidentally identical to one of our previously detected mutations,[4] further confirming its relationship to disease.

The other genetic defect that we identified in this individual is a polyalanine length variation in the *PHOX2B*. We previously reported that constant exotropia displays a marked association with schizophrenia ($P = 0.00000000906$, odds ratio (OR) = 20.6, 95% CI 4.83–87.8), and that deletion/insertion polymorphisms in the 20-alanine homopolymer stretch of *PHOX2B* disturbs its transcription.[5] We detected a modest association between these functional polymorphisms and all those with schizophrenia ($P = 0.012$, OR = 1.59, 95% CI 1.01–2.50) and those with schizophrenia and constant exotropia ($P = 0.004$, OR = 4.52, 95% CI 1.78–11.5).[5]

In summary, we propose a combinatorial model for the genetic risk of schizophrenia where the combination of a CNV, in this case 22q11.2DS, with a large effect; a *GLO1* frameshift mutation with a probable moderate to large effect; and a 5-alanine deletion with a modest effect, collaborate to exceed a developmental threshold for the onset of schizophrenia. This proposal is the first discrete evidence for a multiple-hit hypothesis in schizophrenia, and although the current findings are fortuitous, the emerging availability of whole genome sequencing methodologies in the near future should help to systematically decipher the detailed genetic mechanisms that determine which individuals who are schizophrenia-associated CNV carriers go on to develop the disease, and to define its precise genetic spectrum.

M. Toyosima, PhD, **M. Maekawa**, MD, PhD, **T. Toyota**, MD, PhD, **Y. Iwayama**, MS, Laboratory for Molecular Psychiatry, RIKEN Brain Science Institute, Saitama; **M. Arai**, PhD, **T. Ichikawa**, MD, **M. Miyashita**, PhD, Project for Schizophrenia Research, Tokyo Institute of Psychiatry, Tokyo; **T. Arinami**, MD, PhD, Department of Medical Genetics, Graduate School of Comprehensive Human Sciences, University of Tsukuba, Tsukuba, Ibaraki; **M. Itokawa**, MD, PhD, Laboratory for Molecular Psychiatry, RIKEN Brain Science Institute, Saitama, and Project for Schizophrenia Research, Tokyo Institute of Psychiatry, Tokyo; **T. Yoshikawa**, MD, PhD, Laboratory for Molecular Psychiatry, RIKEN Brain Science Institute, Saitama, Japan

Correspondence: Motoko Maekawa, Laboratory for Molecular Psychiatry RIKEN Brain Science Institute, 2-1 Hirosawa, Wako-city, Saitama 351-0198, Japan. Email: mmaekawa@brain.riken.jp

First received 3 Mar 2011, final revision 10 May 2011, accepted 16 Jun 2011

Funding

This work was supported by RIKEN BSI Funds, and a part of this study is the result of 'Development of biomarker candidates for social behavior' carried out under the Strategic Research Program for Brain Sciences by the MEXT of Japan.

References

1 Karayiorgou M, Simon TJ, Gogos JA. 22q11.2 microdeletions: linking DNA structural variation to brain dysfunction and schizophrenia. *Nat Rev Neurosci* 2010; **11**: 402–16.

2 American Psychiatric Association. *Diagnostic and Statistical Manual of Mental Disorders (3rd edn, revised) (DSM–III–R)*. APA, 1987.

3 Arinami T, Ohtsuki T, Takase K, Shimizu H, Yoshikawa T, Horigome H, et al. Screening for 22q11 deletions in a schizophrenia population. *Schizophr Res* 2001; **52**: 167–70.

4 Arai M, Yuzawa H, Nohara I, Ohnishi T, Obata N, Iwayama Y, et al. Enhanced carbonyl stress in a subpopulation of schizophrenia. *Arch Gen Psychiatry* 2010; **67**: 589–97.

5 Toyota T, Yoshitsugu K, Ebihara M, Yamada K, Ohba H, Fukasawa M, et al. Association between schizophrenia with ocular misalignment and polyalanine length variation in PMX2B. *Hum Mol Genet* 2004; **13**: 551–61.

6 Vassos E, Collier DA, Holden S, Patch C, Rujescu D, St Clair D, et al. Penetrance for copy number variants associated with schizophrenia. *Hum Mol Genet* 2010; **19**: 3477–81.

7 Thornalley PJ. The glyoxalase system in health and disease. *Mol Aspects Med* 1993; **14**: 287–371.

EXTRA CONTENT ONLINE

シンポジウム　精神医学研究の到達点と展望*

脳科学研究から見えてきた統合失調症の病態および治療と予防の展開**

糸川昌成[1,3,4]　新井　誠[1]　小池進介[1,2]　滝沢　龍
市川智恵[1]　宮下光弘[1,3]　吉川武男[4]　宮田敏男[5]
笠井清登[2]　岡崎祐士[1,3]

Key words

Carbonyl stress, Schizophrenia, Preventive medicine

はじめに

統合失調症は，遺伝率(heritability)が0.8，λs(同胞間の相対危険率)が8.2(I型糖尿病15，アルツハイマー病4～5)と，遺伝要因が大きい疾患である(表1)。そこで，原因解明には遺伝学的アプローチが有望であると考えられてきた。90年代は，連鎖解析で位置的(positional)に染色体上の座位を決めて原因遺伝子をクローニングする研究が流行した。こうした研究は，主としてメンデル型遺伝形式をとる単一遺伝子疾患で成果を挙げたが，統合失調症でも同様の挑戦がなされdysbindinやneuregulin1など有望な遺伝子が同定された。しかし，その後の研究で，関連するSNP(single nucleotide polymorphism)が報告者間で異なる，あるいはSNPが一致してもリスクアレルが報告者によって逆向きであるといった不透明な結果が続いている。一方，近年は生活習慣病のような多因子疾患で，common disease-common variant仮説に基づいて，全ゲノム関連解析(genome-wide association study；GWAS)が行われている。統合失調症を対象としたGWASでも，

2011年4月25日受稿，2011年11月8日受理

* 第39回精神研シンポジウム(2010年11月)より

** Perspective of Pathophysiology, Therapeutics and Prevention of Schizophrenia from Point of the View of Brain Sciences

1) 東京都医学総合研究所統合失調症・うつ病プロジェクト(〒156-8506 東京都世田谷区上北沢2-1-6)，Itokawa Masanari, Arai Makoto, Koike Shinsuke, Takizawa Ryu, Ichikawa Tomoe, Miyashita Mitsuhiro, Okazaki Yuji：Project for Schizophrenia and Affective Disorders Research, Tokyo Metropolitan Institute of Medical Science, Tokyo, Japan
2) 東京大学医学部附属病院精神神経科，Kasai Kiyoto：Department of Psychiatry, Tokyo University
3) 東京都立松沢病院精神科，Department of Psychiatry, Tokyo Metropolitan Matsuzawa Hospital
4) 理化学研究所脳科学総合研究センター分子精神科学研究チーム，Yoshikawa Takeo：Lab. for Molecular Psychiatry, Brain Science Institute, RIKEN
5) 東北大学大学院医学系研究科付属創生応用医学研究センター，Miyata Toshio：Center for Translational and Advanced Research on Human Disease, Tohoku University Graduate School of Medicine

0488-1281/11/¥500/論文/JCOPY

表1 統合失調症の相対危険率とGWASで同定された遺伝子のオッズ比

Risk ratio[a]	Obserbed	GWAS		
		Odds ratio	gene	
λ_O	10.0			
λ_S	8.6			Rich 1990
λ_M	52.1			
λ_D	14.2			
		1.10	*ZNF804A*	Williams et al. 2010
		1.16	CACNA1C	Nyegaard et al. 2010
		1.87	*JARID2*	Liu et al. 2009
		1.22	*GENTG2*	
		1.25	*NTRK3*	
		1.68	*DDX31*	Jianxin et al. 2009
		2.02	*RNLS*	
		1.64	*GTF3C4*	
		1.30	*TRPA1*	
		1.15	*HIST1H2B*	
		1.20	*PRSS16*	
		1.24	*PGBD1*	Stefansson et al. 2009
		1.15	*NRGN*	
		1.23	*TCF4*	
		1.41	*RELIN*	Shifman et al. 2008

[a] Definitions of subscripts : O=offspring ; S=siblings ; M=MZ twins ; D=DZ twins

いくつかの感受性遺伝子が報告されているが，いずれのオッズ比も1.5前後と小さい(表1)。遺伝率やλsは十分大きいのに，同定される感受性遺伝子は効果の小さいものばかりである。このようなmissing heritabilityを克服しようとして，最近の研究では数千の検体数と数十万のSNPを解析するに至っており，欧米では研究規模が競い合われるようにして拡大されている。

筆者らは，主として欧米で取り組まれている国家プロジェクト級のビッグサイエンスとは違ったアプローチを考え，以下の2点を工夫した。①遺伝子解析だけでなく生化学的解析を組み合わせ，②まれだが大きな遺伝子効果をもたらす変異を同定し，それをプロトタイプとして一般症例に敷衍する。上記2つを実施した結果，興味深い成果を得たので本稿にて紹介する。本研究は東京都精神医学総合研究所および関連施設の倫理委員会の承認を得て，被験者にインフォームドコンセントののち書面にて同意を得て行われた。

まれな遺伝子変異の同定

まれで比較的大きな遺伝子効果をもたらす変異は，単一遺伝子疾患に近い遺伝形式をとることを想定し，まず多発家系に注目した。機能変化の大きい変異はまれで新規であると考え，候補遺伝子の全塩基配列を解読するresequenceを実施した。候補遺伝子には，連鎖解析研究により複数のグループから統合失調症との連鎖が報告されている6番染色体短腕6p21[4,6,12]に注目し，ここにコードされている*glyoxalase I*(*GLO1*)を選択した。GLO1は，酸化ストレスなどで生じる有害なカルボニル化合物を分解解毒する酵素であり，発現量の違いが情動に影響することも報告されていた[5]。多発家系の発端者ばかり約50例でresequenceを行った結果，1例から*GLO1*遺伝子のexon1にadenineが1塩基挿入する新規のフレームシフト変異を同定した。症例の家系には，3親等内に同胞全員を含め5名の統合失調症罹患者がいた。症例の*GLO1*遺伝子ではフレームシフ